Investigating mutants of the PilA helix in *Pseudomonas aeruginosa*

A Thesis submitted to
Indian Institute of Science Education and Research Pune
in partial fulfilment of the requirements
for the BS-MS Dual Degree Programme

by

Anjali Pattathil

Indian Institute of Science Education and Research Pune

Dr. Homi Bhabha Road,

Pashan, Pune 411008, INDIA.

April, 2025

Supervisor: Alexandre Persat

Anjali Pattathil

Certificate

This is to certify that this dissertation entitled "**Investigating mutants of the PilA helix in *Pseudomonas aeruginosa***" towards the partial fulfilment of the BS-MS dual degree programme at the Indian Institute of Science Education and Research, Pune represents study/work carried out by Anjali Pattathil at Indian Institute of Science Education and Research under the supervision of Alexandre Persat, Associate Professor, SV, during the academic year 2024-2025.

Anjali Pattathil	Alexandre Persat	Sunish Radhakrishnan
(IISER Pune)	(EPFL)	(IISER Pune)
20201018	Supervisor	Expert

This thesis is dedicated to instant ramen

Declaration

I hereby declare that the matter embodied in the report entitled "**Investigating mutants of the PilA helix in *Pseudomonas aeruginosa***" are the results of the work carried out by me at the Department of Life Sciences, École Polytechnique Fédérale de Lausanne (EPFL), under the supervision of Alexandre Persat, and the same has not been submitted elsewhere for any other degree. Wherever others contribute, every effort is made to indicate this clearly, with due reference to the literature and acknowledgement of collaborative research and discussions.

Anjali Pattathil

(IISER Pune)

20201018

Table of Contents

List of Tables

List of Figures

List of Abbreviations

AMR - Antimicrobial Resistance

BACTH - Bacterial adenylate cyclase two-hybrid

BPPL - Bacteria Pathogen Priority List

cAMP - Cyclic adenosine monophosphate (cyclic AMP)

Carb - Carbenicillin

CyaB - Adenylyl cyclase B

EPS - Extracellular polymeric substances

ESKAPE - *Enterococcus faecium, Staphylococcus aureus, Klebsiella pneumoniae, Acinetobacter baumannii, Pseudomonas aeruginosa* and *Enterobacter* spp.

Gm - Gentamicin

LB - Lysogeny broth (or Luria-Bertani medium)

LBD - Ligand-binding domain (of MCPs)

MCP - Methyl-accepting chemotaxis protein

MDR - Multi-Drug Resistance

MOI - Multiplicity of Infection

OD_{600} - Optical density (measured for the wavelength of 600nm)

PCR - Polymerase Chain Reaction

SD - Signalling Domain (of MCPs)

TFP (or T4P) - Type IV pili

Vfr - Virulence factor regulator

WT - Wild-Type

Acknowledgements

I would like to thank my supervisor, Dr Alexandre Persat, for allowing me to pursue this project in his group. It is an incredibly vibrant and nurturing scientific environment, and I will treasure my experience here forever. I also want to thank my expert, Dr Sunish Radhakrishnan, for all.his advice and knowledge of the field.

I want to thank all my labmates for their support and kindness – learning from their competence and creativity was an honor. I'm grateful especially to Zainebe Al-Mayyeh for making the transition to a new country and an unfamiliar lab so much easier.
I want to thank Alice Pellegrino and Dea Müller for material support with the phage and twitching assays, Miro Plum and Sourabh Monnappa for their advice with presentation, and Sourabh again for letting me into the lab that one time.
I want to thank my mentor, Chia-Ni Tsai, for everything, but especially for her endless patience. Learning microscopy and image analysis was a steep curve for me, and she had to explain many things multiple times.

I want to thank Dr Amrita Hazra, Aditya Bhattacharya and Dr Mehmet Berkmen for informing so much of my approach to research and writing.
I'm grateful for the support of my family for the past year; there were many challenges that would likely have been far more challenging without them.

Finally, I'm grateful to Krish and Khushi. For being my home wherever we ended up. I can never thank you enough.

Abstract

Type IV pili are a vital component to bacterial surface sensing. It is a polymer that is composed of the major pilin PilA – it extends from the surface of the cell, attaches to a surface and pulls the cell forward upon retraction. This motion is called twitching motility. The retraction of the Type IV pilus forms the core of a major surface-sensing mechanism.

The PilA protein has an alpha-helical domain that sits at the core of the pilus and serves a number of functions – it is theorised to contribute to the “stretchability” of the pilus and its ability to withstand tensile force. It has also been implicated in signalling events that help the cell switch to a superficial lifestyle, and the upregulation of virulence factors.

The domain contains two helix-breaking residues that flank a short stretch of amino acids that unfold from an alpha-helical conformation in an assembled pilus.

In this study, random mutagenesis was used to mutate the two helix-breaking residues of the alpha-helical domain of PilA in *Pseudomonas aeruginosa*. The effect of these mutations were tested for pilus formation, motility and signalling. Large and/or charged residues disrupt the formation or functioning of the pilus, but single mutations to small non-polar residues retain quite a lot of the original function. The P22 residue especially appears to absorb mutations well. Two double mutations were also attempted, but they exhibited no functionality at all. Signalling phenotypes matched the twitching phenotypes closely for a small sample of the mutants, suggesting that they follow from one another.

It is clear that neither of the two residues are independently essential to pilus assembly or signalling, but further study will be required to understand the true structural impact of these mutations.

Introduction

1.1 *Pseudomonas aeruginosa*

In 1882, the French pharmacist Carle Gessard published “On the Blue and Green Coloration that Appears on Bandages”, describing a microscopic organism that produced a blue-green compound called pyocyanin. It was isolated from bandage linens, and while he does some preliminary characterisation of the organism itself, Dr Gessard spends most of his short note studying the properties of the compound instead[1]. This is the first known isolation of the bacterium that would come to be known as *Pseudomonas aeruginosa*[1, 2].

He went on to study his discovery further, and actually named the genus *Pseudomonas* to include all gram-negative aerobic bacilli with polar flagella. This had to later be adjusted for specificity[2], and because the species can survive without oxygen[3].

Its genome was sequenced by Stover et al. in 2000 [4]. At the time, it was the largest sequenced bacterial genome by a significant measure.

In the current day, *P.aeruginosa* is known as an opportunistic pathogen and extremely versatile organism. It’s been isolated from a range of infectious and environmental conditions, and can survive on a vast number of carbon substrates[4]. It is intrinsically resistant to several antimicrobials[4], and the carbapenem-resistant strain has been on the WHO Bacteria priority pathogen list (BPPL) since it was first published in 2017[5].

It is one of the ESKAPE pathogens, a group of six bacterial pathogens (*Enterococcus faecium, Staphylococcus aureus, Klebsiella pneumoniae, Acinetobacter baumannii, Pseudomonas aeruginosa* and *Enterobacter* spp.) that are known to be highly virulent, opportunistic and resistant to antibiotics[6]. They are all common suspects worldwide in nosocomial (hospital-acquired) infections, in part due to their ability to form protective biofilms.

1.2 Biofilms and Surface-sensing

Biolfilms represent superficial bacterial communities that sit in an extracellular matrix of their own making. It is a distinct way of life from bacteria that are planktonic, or free-floating, in a liquid medium[7]. Biolfilms are among the most successful approaches to life on earth; we have observed them in most known environments, from deep-sea hydrothermal vents to the inside of medical devices. They are extremely resilient to most forms of stress – predation, toxins, radiation and so on. It allows for efficient storage and distribution of nutrients, and stability in terms of location[7,8].

Medically, biofilms are notorious for being incredibly widespread, resilient to immune clearance, and resistant to traditional forms of therapy, like antibiotics. They are noted for their role in chronic bacterial infection[7]. The ESKAPE pathogens in particular have many other mechanisms of AMR, but biofilms are a time-honored strategy.

The matrix acts as a physical obstacle to many antimicrobials, and the complex chemical environments within them can hinder their activity as well[7].

Since their discovery in 1978[9], we have learned a great deal about biofilms. The recent rise of multidrug-resistant pathogens, particularly, has spurred a vast amount of research in the field, but a lot remains to be found. Understanding their nature and the process of their formation could hold the key to any number of new treatments in the age of MDR pathogens.

The first step in biofilm formation for any organism is surface-sensing. It is only once they sense the presence of a surface that they can attach to it and begin to proliferate as a colony. This process is associated with a number of physiological and morphological changes across various timescales (cAMP signalling, EPS production, production of virulence factors in infectious strains and so on [10, 11]).

Surface-sensing mechanisms are yet to be perfectly understood, but they rely both on chemical [12, 13] and mechanical cues, with the mechanical cues coming from appendages like Type IV pili (TFP)[14] and flagella[15]. Major players of the

subsequent signalling process, like the Pil-Chp and Wsp chemosensory systems, have also been identified[16, 17].

This work focuses on TFP-mediated mechanisms in Pseudomonas aeruginosa (strain PAO1).

1.3 Type 4 Pili – structure and function

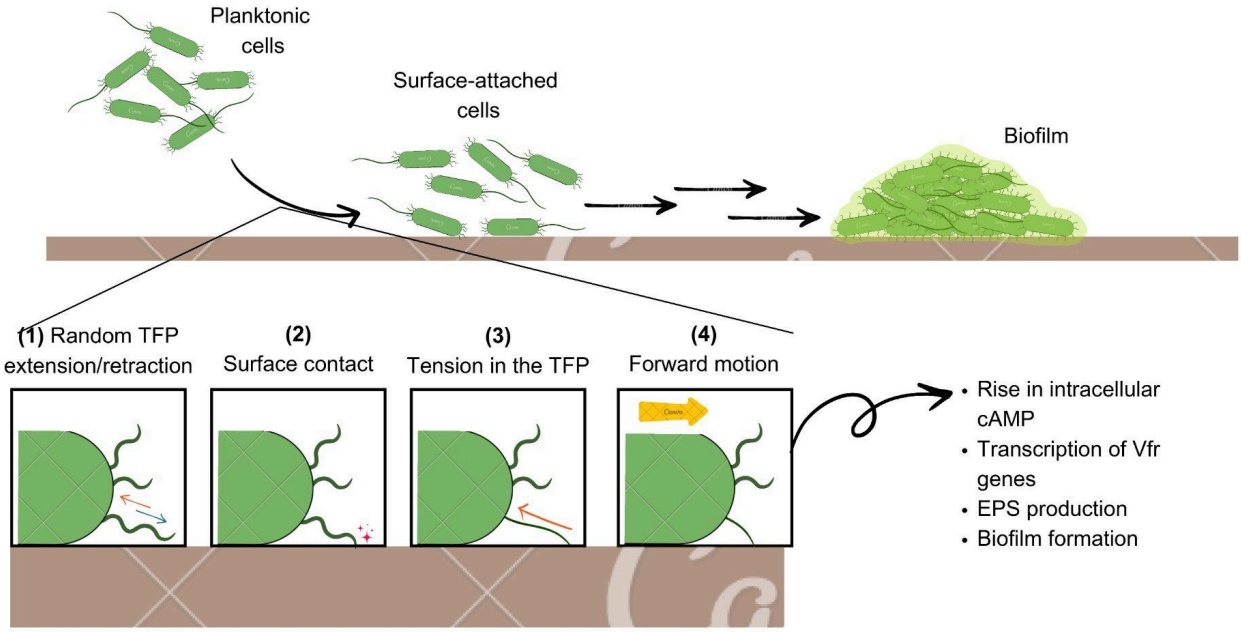

Figure 1 – TFP-mediated surface-sensing. **(1)** Type IV pili extend and retract randomly. **(2)** They contact and attach to a surface. **(3)** Upon retraction, tensile force is generated in the pilus, which **(4)** pulls the cell forward. On multiple timescales, from several minutes to hours, downstream effects are triggered.

Type IV Pili (abbreviated to T4P or TFP) are filamentous polymers that are assembled largely from the pool of pilin monomers found in the inner membrane of the bacterium. The scaffolding platform proteins can attach to both the assembly and the retraction ATPases (PilB and PilT respectively), which polymerise and depolymerise the pilin monomers respectively[17, 18]. The major pilin monomer in *P.aeruginosa* is the PilA protein. There are also minor pilins (like PilE, PilX and PilW) that play various roles in initiating assembly and aiding the function of the TFP[35].

TFP extend and retract stochastically, and upon encountering a surface, the pilus attaches to it[19]. The bacteria is pulled forward by the tensile force generated in the pilus when it retracts, in a particular motion known as twitching motility[Figure 1]. A bacteria without pili cannot twitch, and neither can a bacteria that cannot retract its pili. PilT deletion mutants have high numbers of abnormally long pili that cannot retract upon surface contact; they cannot twitch[20].

The TFP retraction motor PilT is the most powerful known molecular motor[21]. Maier et al. (2002) [22] measured the generation of forces well over 100pN by single motors in *N.gonorrhoeae*.

Upon contact, how exactly the signal is transmitted remains unknown (as well what it is), but the inner membrane protein PilJ has been shown to interact directly with PilA[23]. PilJ is a methyl-accepting chemotaxis protein (MCP), one of a very common class of bacterial and archaeal receptors, typically involved in the sensing of environmental cues. They differ significantly in their periplasmic ligand-binding domains (LBD), but have a much higher degree of conservation in their cytosolic signalling domains (SD). There are also entirely cytosolic MCPs, but those are more common in archaea[24].

The interaction between PilA and PilJ was demonstrated through BACTH fusions by Persat et al. in 2015 [23] – and that it likely happened between the transmembrane domains of both proteins.

One theory for the mechanism of signalling is that the pilus physically deforms or stretches upon being subjected to tensile force, and this “stretched” conformation is sensed by proteins like PilJ. Biais et al. (2010) [25] used molecular combing to artificially stretch purified TFP from *Neisseria gonorrhoeae*, and used Transmission electron microscopy (TEM) to visualise the clear difference between stretched and unstretched fibres. The magnitude of the force used to accomplish this was at the upper limit of those encountered in real life, but nevertheless, it may differ in profile from forces in *in vivo* conditions.

Another theory is that pilus retraction causes a small local spike in PilA concentration at the base of the pilus, and this change is sensed by signalling proteins like PilJ. The local spike has been shown using fluorescent microscopy on maleimide-labelled PilA[26], but maleimide labelling has been shown to interfere with TFP assembly and motility[17, 27]. Persat et al. (2015) used microfluidic channels to subject the pili of a *ΔPilT* mutant to tensile force without allowing retraction, and showed that it did not trigger downstream signalling any more than the control. This demonstrates that retraction is necessary, but may not be sufficient[23]. They note that the small amount of signaling observed could be the result of small random mechanical perturbations.

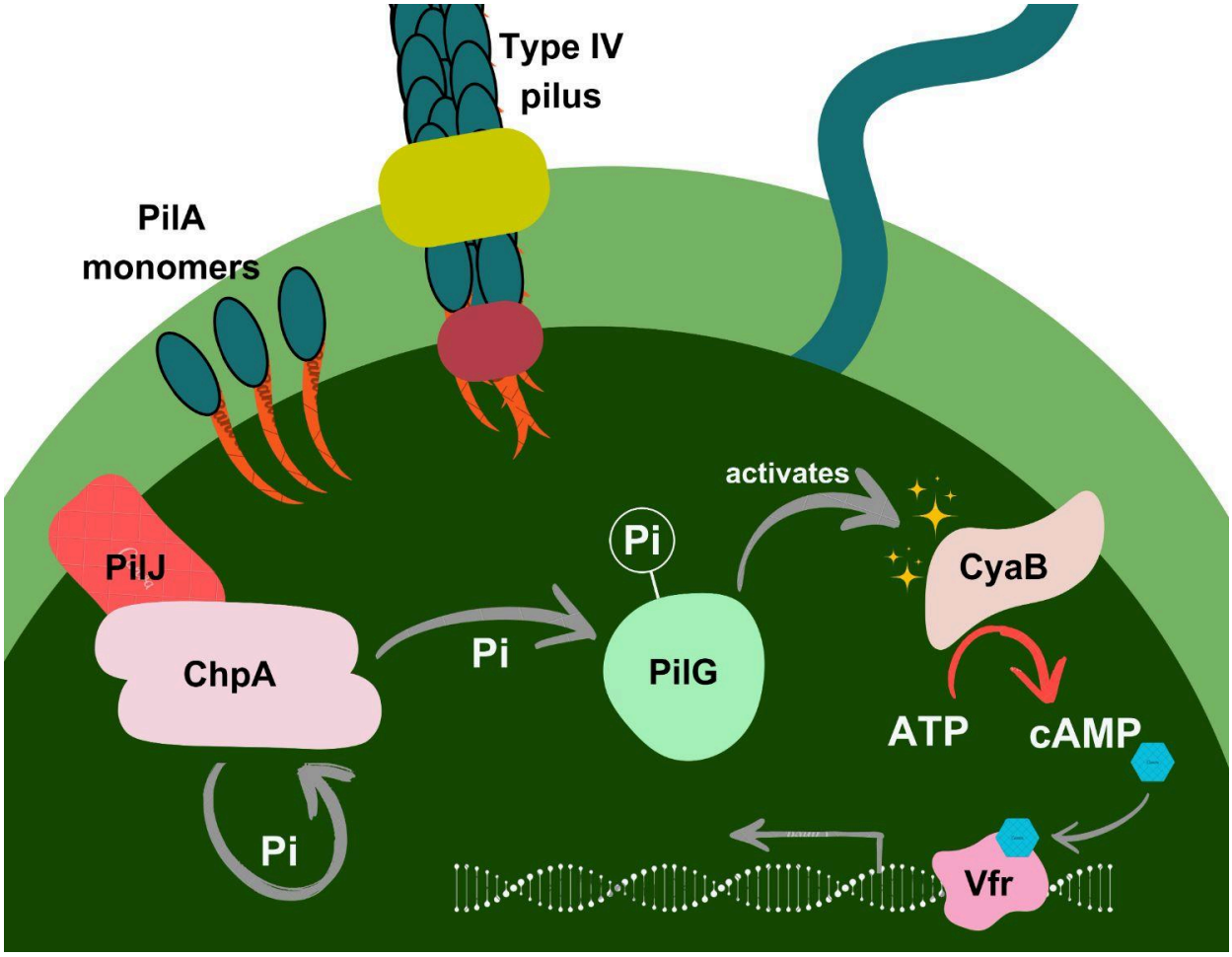

Figure 2 – Pil-Chp signalling.

As illustrated in Figure 2, PilJ (or a different unidentified player) subsequently transmits the signal to the histidine kinase ChpA. Following this, the signal is transduced by a phosphorelay – ChpA autophosphorylates, then transfers a phosphate group to PilG. Phospho-PilG activates the adenylyl cyclase CyaB, which in turn increases the amount of intracellular cAMP. cAMP upregulates the transcriptional regulator Vfr (virulence factor regulator), which controls the expression of over a hundred genes, all variously involved with further adhesion, biofilm formation and pathogenesis. Type IV pili production is upregulated upon surface sensing[20], as is the *xphA-xqhA* operon, commonly known as the *PaQa* operon[26].

It should be noted here that this phenomenon is polar, Pseudomonas can sense surfaces at one pole or the other. PilH, the negative regulator of CyaB, is the counterpart of PilG. It facilitates its ability to change direction upon encountering an obstacle, called contact reversal. Deletion mutants lose this ability[28].

Mutants of the Pil-Chp system tend to downregulate the TFP machinery altogether, so the defects in motility caused by them are often challenging to study[28].

1.4 PilA

The PilA protein, or the major pilin, is 149 amino acids long, and has two domains, the N-terminal α-helix and the C-terminal β-sheet. The helices form the core of the pilus, while the β-sheets coat the outside of the filament. Correspondingly, the helix residues are broadly more hydrophobic than the β-sheet residues [29].

Near the centre of the helix, there is a short stretch of amino acids that appears to melt only when the monomer is inserted into a pilus, and otherwise forms part of the helix i.e. the structure of the monomer differs when it is imaged as a monomer versus a polymer. The prevailing understanding of the cause of this melting is the two amino acid residues that (roughly) flank this stretch – G14 and P22. Glycine and proline are referred to as helix-breaking residues – glycine is too flexible to fit into a helix and proline is constricted to an unfavorable angle[30, 31]. The details of the structure are illustrated in Figure 3.

These residues, along with some others, are extremely conserved in TFP[30]. Their role and the role of the region is debated. They may destabilise the helix of the monomer and allow it to melt upon integration into a pilus. It could also serve a functional role in the stretching of the pilus upon attachment and retraction, or as a binding site for downstream signalling molecules like PilJ.

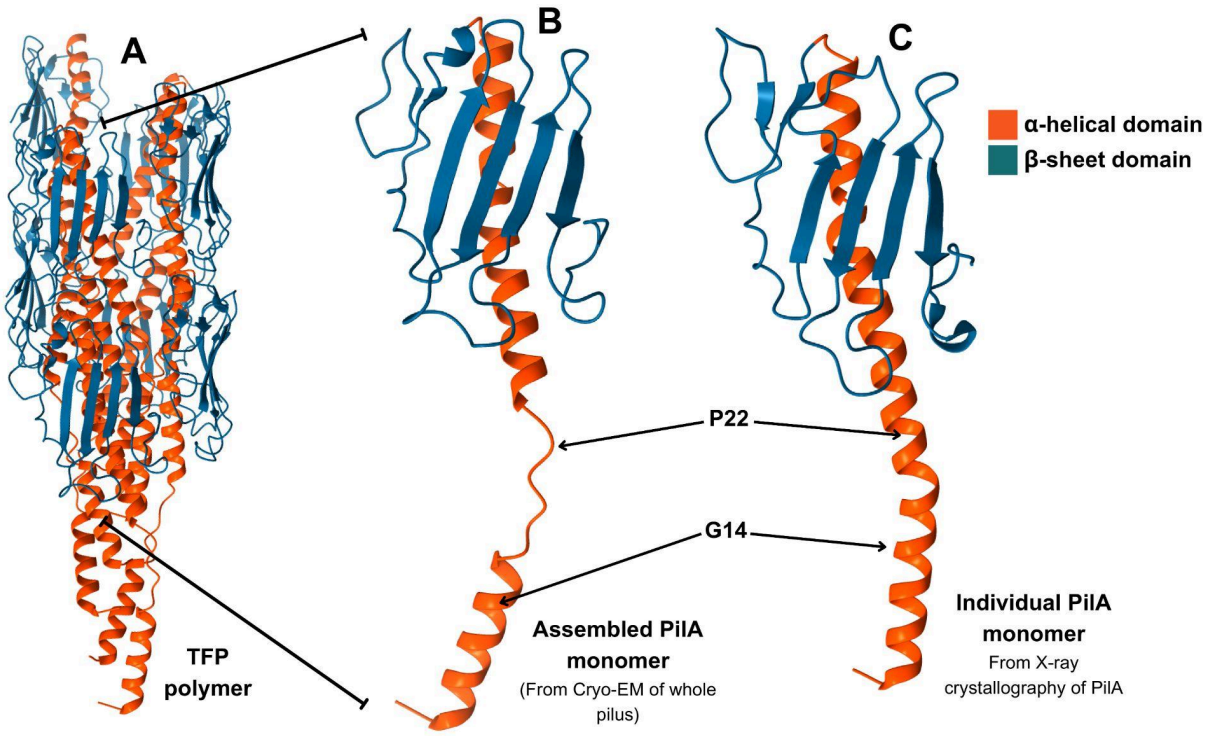

Figure 3 – Structure of PilA and the Type IV pilus. (A) The Type IV pilus polymer, comprised of PilA monomers, with its helices (orange) facing the core and β-sheets (blue) facing the outside. **(B)** The major pilin PilA has two domains - the α-helix and the β-sheet. This is derived from a Cryo-EM image of the PAO1 TFP polymer[31], and shows the melted region between G14 and P22 **(C)** X-ray crystallography-derived image of PilA[29] from the PAK strain, lacking the melted region.

Wang et al. published cryoelectron microscopy reconstructions in 2017 [30] of the assembled *N.gonorrhoeae* and P.aeruginosa (strain PAK) TFP, accompanied with some mutational studies (on the PilA-equivalent gene of *N.meningitidis* - PilE) of residues they felt might be structurally relevant, which included G14 and P22. Alanine mutants of both

had far fewer pili, but P22 had almost none, leading to their conclusion that P22 played a critical role in pilus assembly.

Kuchma and O'Toole (2022) [20] studied mutants of PilA in the PA14 strain of *P.aeruginosa*, and found that the P22A mutation interfered with motility, likely due to issues with assembly. They also showed that the mutant had a higher affinity to PilJ, but a lower final cAMP response, though this could be an experimental artefact.

1.5 Scope of the Study

To make a concerted effort to understand what the role of this region may be, random mutants were made of the two helix-breaking residues in strain PAO1 of *P.aeruginosa*. These mutants were then tested for changes in motility and signalling, to see if –

- If it is possible to replace one or both residues without entirely disrupting the structure and/ or functioning of the pilus.
- If the defects would be coupled i.e. could there be such a thing as a mutant that showed a twitching defect and not a signalling defect. This would imply that the residues had more than a single role.

Our knowledge of the structure-function relationship of PilA remains woefully incomplete, given its centrality to the virulence of several bacterial pathogens. This project was intended to fill in a part of it.

Materials and Methods

2.1 Materials

2.1.1 Reagents and Media

Material	Supplier
Media and Media components	
LB	Carl Roth
Tryptone	Carl Roth
Agarose	Carl Roth
NaCl	Fisher Scientific
Agar	Fisher Scientific
Antibiotics	
Gentamicin	BioChemica
Carbenicillin	Fisher Scientific
Cloning reagents	
Primers	Microsynth
Pfu polymerase and 5X buffer	Thermo Scientific
dNTPs	Thermo Scientific
Restriction enzymes and buffers	NEB
DNA ladder and dye	Thermo Scientific
CYBR Safe gel stain	Invitrogen
Gibson assembly Mastermix	NEB

GoTaq Green 2X mastermix (for colony PCR)	Promega
Gel extraction kit	NEB
Miniprep kit	Thermo Scientific
Miscellaneous	
DMSO	Fisher Scientific
D(+) - Sucrose	PanReac

Table 1 – Reagents and media

2.1.2 Strains

Escherichia coli strain XL10 was used for all the cloning and plasmid construction.

Pseudomonas aeruginosa strain PAO1 was used as the parental strain for all experimentation. Lab-made strains of PAO1*ΔFliC* and PAO1*ΔFliCΔPilA* were used in actuality, following electroporation with the relevant plasmids. The first was brought to the lab by Alexandre Persat, and the second was constructed by Zainebe Dhirani and Marco Kühn, members of Persat lab.

Strains used for the phage assay were PAO1*ΔFliCΔPilU*, PAO1*ΔFliCΔPilB*, PAO1*ΔFliCΔPilG*, PAO1*ΔFliCΔPilTΔPilU*, all brought from Zemer Gitai's lab by Alexandre Persat.

Also used were PAO1*ΔFliCΔPilJ* (constructed by Marco Kühn and Zaïnebe Dhirani, Persat lab), PAO1*ΔFliC PilA_A86C* (Marco J Kühn, Persat lab) and PAO1*ΔFliC PilT_D160N* (Zaïnebe Dhirani, Persat lab).

Growth was done in LB media or LB-agar plates at 37°C, for both *P.aeruginosa* and *E.coli*. Antibiotics were added depending on the resistance of any plasmids that the strain contained – 300µg/mL of carbenicillin and 60µg/mL of gentamicin for PAO1 and 10µg/mL of gentamicin for XL10.

Specialised plates were made for the phage titre assay, single-cell twitching, twitching stab assay and the *PaQa* assay – the recipes are given below in the concerning sections.

2.1.3 Plasmids

The PilA gene was mutated and supplemented back to the PAO1*ΔFliCΔPilA* strain on the pJN105 plasmid, with its own promoter on the same plasmid. This was constructed by Xavier Pierrat, a previous member of the lab. It carries a gentamicin resistance gene. The reporter for the *PaQa* operon was cloned into the pUCP18 plasmid by Alexandre Persat. It carries a carbenicillin resistance gene.

2.2 Experimental Methods

2.2.1 Cloning or Plasmid construction

Cloning was accomplished using Gibson assembly[31]. The primer pairs – (P1, P4), (P2, P3), (P1, P6), (P2, P5) – were used to expand randomly mutated versions of the PilA gene from the WT version of the gene, which had been cloned, along with the WT PilA promoter, into the pJN105 vector. The PCR mixture would be run on a 1% agarose gel, and the correct bands would be purified using gel extraction.

The two corresponding fragments were subsequently stitched together by Gibson assembly with the linearised empty vector. The fragments had a 15-20bp overlap for this purpose, created by adding them to the 5'-end of the primers.

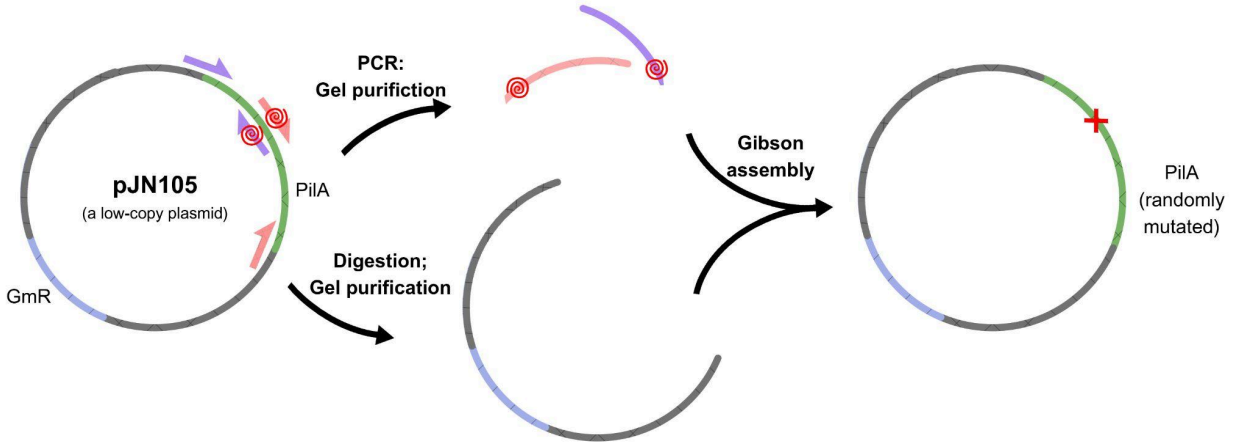

Figure 4 – Cloning protocol. Two fragments are generated with PCR, which overlap with each other and with the backbone. They are joined with the digested plasmid backbone using Gibson assembly.

The primers designed for the double mutants (P7, P8), (P9, P10) were designed for specific mutations (P22A and P22V), and were not randomised. The starting template for each was the G14A and G14V mutants of the gene.

The Gibson assembly mixture would be transformed into chemically competent XL10 cells. All the colonies would be tested the following day using colony PCR with primers flanking the PilA gene and promoter (P11 and P12). The bands would be purified and sent for sequencing. Any colonies that were correctly mutated would be cultured. The plasmids were extracted from them, and sent for a final round of sequencing. If there were no unwanted mutations, the plasmids would be electroporated in competent PAO1*ΔFliCΔPilA* cells, prepared by washing late-exponential cells in 300mM sucrose.

Positive transformants would be identified using colony PCR with the same primers, and a cryostock would be prepared with DMSO (to a final concentration of 10%) for further use.

All primers used for cloning are listed below –

No.	**Primer name**	**Sequence (5'→3')**
1	PilA_termin_F	ggccaccttcgatcaccttagttatca
2	PilA_promo_R	cgtgttggcggaccagcttt
3	PilA_P22X_F	aacatagttctgatactgnnnaatggcaattgccgccaggatac
4	PilA_P22X_R	ctggcggcaattgccattnnncagtatcagaactatgttgcgcgttcg
5	PilA_G14X_F	atggcaattgccgccaggatnnngatgatcgcaaccacgatcatcagttc
6	PilA_G14X_R	tgatcgtggttgcgatcatcnnnatcctggcggcaattgccattc
7	PilA_AA_P22A_F	aacatagttctgatactggcaatggcaattgccgccaggat
8	PilA_AA_P22A_R	ctggcggcaattgccattgcccagtatcagaactatgttgcgcgttcg
9	PilA_VV_P22V_F	aacatagttctgatactgcacaatggcaattgccgccaggat
10	PilA_VV_P22V_R	ctggcggcaattgccattgtgcagtatcagaactatgttgcgcgttcg
11	PilA_seq_F	cgcaactctctactgtttctccataccc

12	PilA_seq_R	gggttttcccagtcacgacgttg

Table 2 – Primers used for cloning and sequencing. Mutagenic sites are marked in red.

Unless mentioned, every strain was made against a PAO1*ΔFliC* background, and every plasmid was transformed into a PAO1*ΔFliCΔPilA* background strain.

2.2.2 Phage titre

Luz19 is a PhiKMV-like lytic virus that attaches to the Type IV pilus, and infects the cell when the pilus is retracted[33, 34]. The efficiency of phage infection can be used as a proxy for the functionality of the Type IV pilus.

Figure 5 – Phage titre measurement. Each row of plaques represent increasing concentrations of Luz19. The countable row is the 10^{-8} dilution, which contains four plaque-forming units. Consequently, the concentration of the original lysate is 4 / (5 ✖ 10^{-3} mL ✖ 10^{-8}) = 8 ✖ 10^{10} pfu/mL. This measurement was performed by Alice Pellegrino.

To find the concentration of virus in cell lysate (denoted by c), soft agar is first prepared, with 0.7g of agar, 2.5g of LB powder in 100mL of distilled water. The solution is

autoclaved and cooled to 55°C in a water bath. 3 (100✖100 mm) square plates are then poured, each containing 30mL of the soft agar and 500µL of an overnight culture of WT PAO1 cells. These are allowed to cool.

A set of fifteen serial dilutions (c ✖ 10^{-1}–10^{-15}) are prepared of the cell lysate, diluted in LB. 5uL of each dilution is spotted on the plate, and the plate is tilted to allow the droplet to spread in a line. After the plate is completely dry, it is left at room temperature overnight.

One or two of the dilutions will contain a countable number of clear plaques on the following day [Figure 5]. This number is used to arrive at the concentration c.

The cell lysate was prepared by Han-Yi Huang, and titre measurements were conducted at various points by Han-Yi Huang, Alice Pellegrino, and myself.

2.2.3 Phage infection assay

To conduct the phage infection assay, the test and control strains are streaked and cultured overnight in 1mL of LB and all relevant antibiotics. The following day, they are diluted 1:200 in 2mL of LB (+ antibiotics), and allowed to grow till they reach an OD_{600} of at least 0.3. If higher, they are diluted to 0.3, and 10µL of the culture is added (in replicates or as needed) to a 96-well plate. 290µL of LB (with or without phage) is added to dilute, to achieve a final MOI (Multiplicity of Infection = no.of phages/no.of bacteria) of 10^{-2} or 10^{-4}, typically. Decreasing the MOI from 10^{-4} was attempted, but trying to add exactly something like 10-100 bacteriophages to each well of a well-plate resulted in noisy data.

The plates were imaged for approximately 20 hours, though only the first ten hours of data is depicted. The plates were shaken (linear, 1440 rpm) every 10 minutes, followed by an OD_{600} measurement. The growth curves were graphed using GraphPad Prism 8.4.3.

For the negative control (a PilA deletion mutant in most instances), the uninfected control grows identically to the infected sample, because the phage has no way to infect the bacterium.

For strains with functioning pili, the cells will grow for a brief period after infection, and then quickly die, causing the OD_{600} to drop significantly, usually to 0. At about 10 or so hours, depending on the strain, the resistant cells will mount a recovery and raise the OD_{600} of the culture again. The uninfected sample, on the other hand, will grow similarly to the PilA- strain.

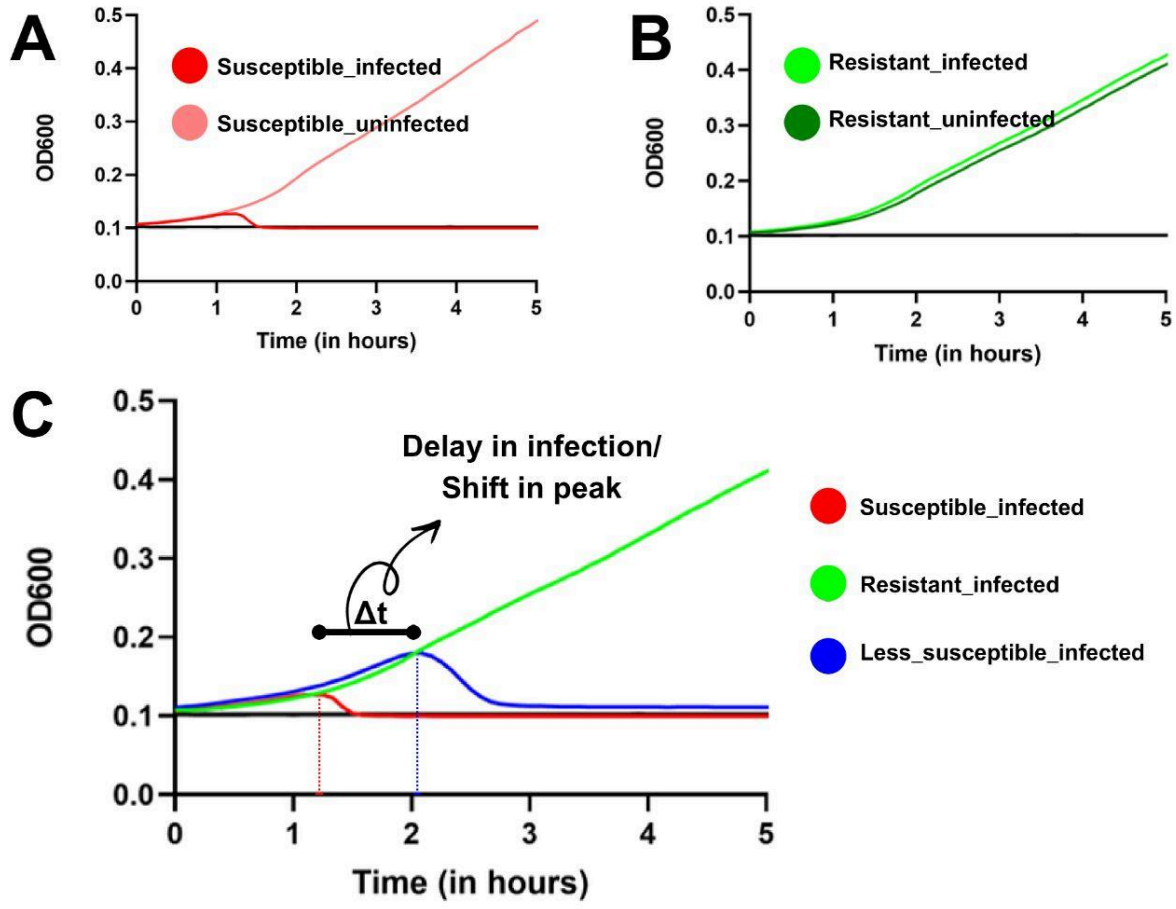

Figure 6 – Phage infection: illustration of growth curves. The above graphs represent the overall layout of the growth curves for a phage infection assay. They are made from real infection data, but do not have error bars or strain names for the sake of simplicity. (**A**) Infection of a strain with WT Type IV pili.

(**B**) Infection of a strain without Type IV pili. (**C**) Infection of a strain with less functional Type IV pili, leading to a delay in the killing peak

In conclusion, susceptible strains have a clear peak of growth prior to virus-induced death. This time is measured and compared to the peak of the WT control, as a metric for the functionality of the TFP.

This metric is not perfect – it does not exactly account for the relative growth rate of the different strains. But as most delays occurred on a timescale of 10-20 minutes, it was deemed sufficient.

2.2.4 Single-cell Twitching

The strains of interest were streaked out (Day 1) and cultured (Day 2) in 1 mL of LB, with appropriate antibiotics. Also on Day 2, TrpCN plates were poured: 0.5g of agarose, 0.5g of tryptone and 0.25g of NaCl were dissolved in 100mL of distilled water and autoclaved. After cooling in a 55°C water bath for 20-25 minutes, 28mL of the media was poured into 3 petri plates (90mm) and allowed to dry for 25-30 minutes. These were stored in the fridge for the next day.

On Day 3, 2 mL secondary cultures were prepared. The first strain was inoculated at a starting OD_{600} of 0.02, and each successive strain had 0.5µL less primary culture than would be required for the same starting OD_{600}. This was done to stagger the growth, so that they would not all reach the correct OD_{600} at the same time. The cultures were allowed to grow for 2-3 hours, until the first strain reached an OD_{600} of 0.2, or slightly higher. An hour or so before this, the plates were taken out of the fridge and allowed to warm in the incubator.

Just prior to sample prep, several pads were stamped out on each plate, with a 16mm round stamp, and a single pad was lifted out using a clean spatula. The culture was diluted to an OD_{600} of 0.2, and 1µL of it was placed on the pad and allowed to dry for 30s. The pad would then be flipped carefully onto a glass-bottomed microscopy dish. Four drops of PBS would be pipetted around the pad in the dish, not touching the pad, to prevent it from drying out during incubation.

After taking an image of the sample, it would be incubated for 2h at 37°C. It would then be imaged again for 5 minutes continuously, with an image taken every 5s. These images were all taken on a Nikon Confocal Scanning microscope at 40X magnification with phase contrast. They were taken at 20% laser power, with an exposure time of 100ms, without binning.

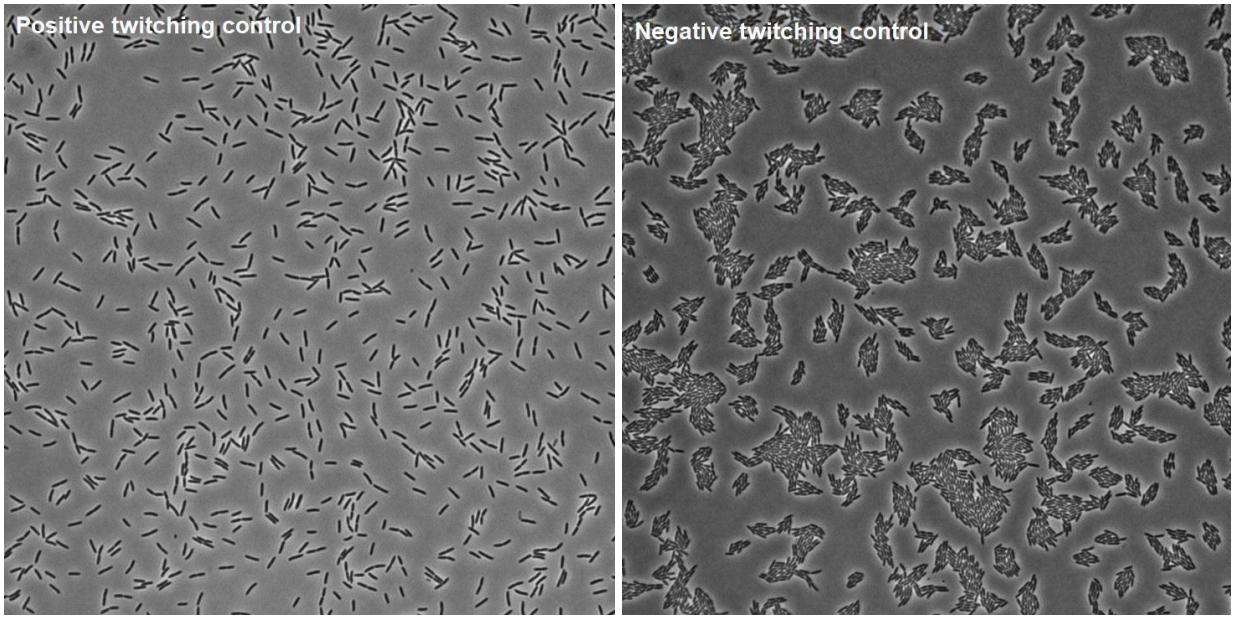

Figure 7 – Stills of positive and negative twitching control strains. These were taken after 2 hours of incubation below an agar pad. **(A)** Positive twitching control – PAO1*ΔFliCΔPilA* pJN105-WT-PilA **(B)** Negative twitching control – PAO1*ΔFliCΔPilA* pJN105 (empty)

As seen in Figure 7, there is a marked difference in cell arrangement in twitching and non-twitching strains. Cells in twitching strains are more evenly spread, because they can move away from each other. Non-twitching strains appear clumped together, because the only thing moving them apart is cell division.

This is not universally true, non-twitching strains sometimes show some intermediate of the two when dividing cells push individual cells out of the main colony. It is, however, a helpful hint.

For quantification, 3-4 random sections of the frame would be chosen so that the cell total was around 100. The chosen cells would be visually observed for the entire duration of 300 seconds, and all cells that showed independent movement in that period would be noted. What that means here is any movement that resulted in the cell changing its location along its long axis, and could not conceivably be said to be caused by contact with surrounding cells.

2.2.5 Twitching stab assay

The strains of interest were streaked out (Day 1) and cultured in LB (Day 2) overnight with appropriate antibiotics.

On the second day, twitching plates were prepared. This assay is quite sensitive to the moisture in the plate, so the recipe and protocol below were followed exactly every time. 1.5g of agarose, 1.5g of tryptone and 0.75g of NaCl were shaken in 300mL of distilled water, in a 500mL bottle. This was autoclaved and taken out when the autoclave had cooled to about 70°C. The bottle was cooled for 20-30 minutes in a 55°C water bath, and 25mL was poured into 11 petri plates, and allowed to dry for exactly 30 minutes. These were then sealed in a plastic bag that was left in the fridge until the following day. The bag would be taken out about an hour before usage, and allowed to warm up in a 37°C incubator.

Meanwhile, the cultures would be diluted 1:100 in the morning in 1mL of LB+antibiotics. This would be allowed to grow for 3-4 hours, till they reached late exponential stage. The culture would all be diluted down to the same starting OD in a small tube. A 10µL tip would be dipped into the diluted culture and stabbed into the twitching plate. This would be done twice more, so that each plate contained three technical replicate stabs of the same strain.

The stabbed plates would be incubated agar side up at 37°C for 17-18 hours. The following morning, the agar would be loosened from the plate by running a 10µL around the edge of the plate. The plate would be held upside down, and the tip would be used to push the agar away from the surface and allow it to drop into a plastic bag open

inside the hood. The empty plate would be allowed to dry open inside the hood until all that is left visible is the imprint of the bacteria. The plates would then be scanned, and the bacterial colonies would be studied for the twitching phenotype.

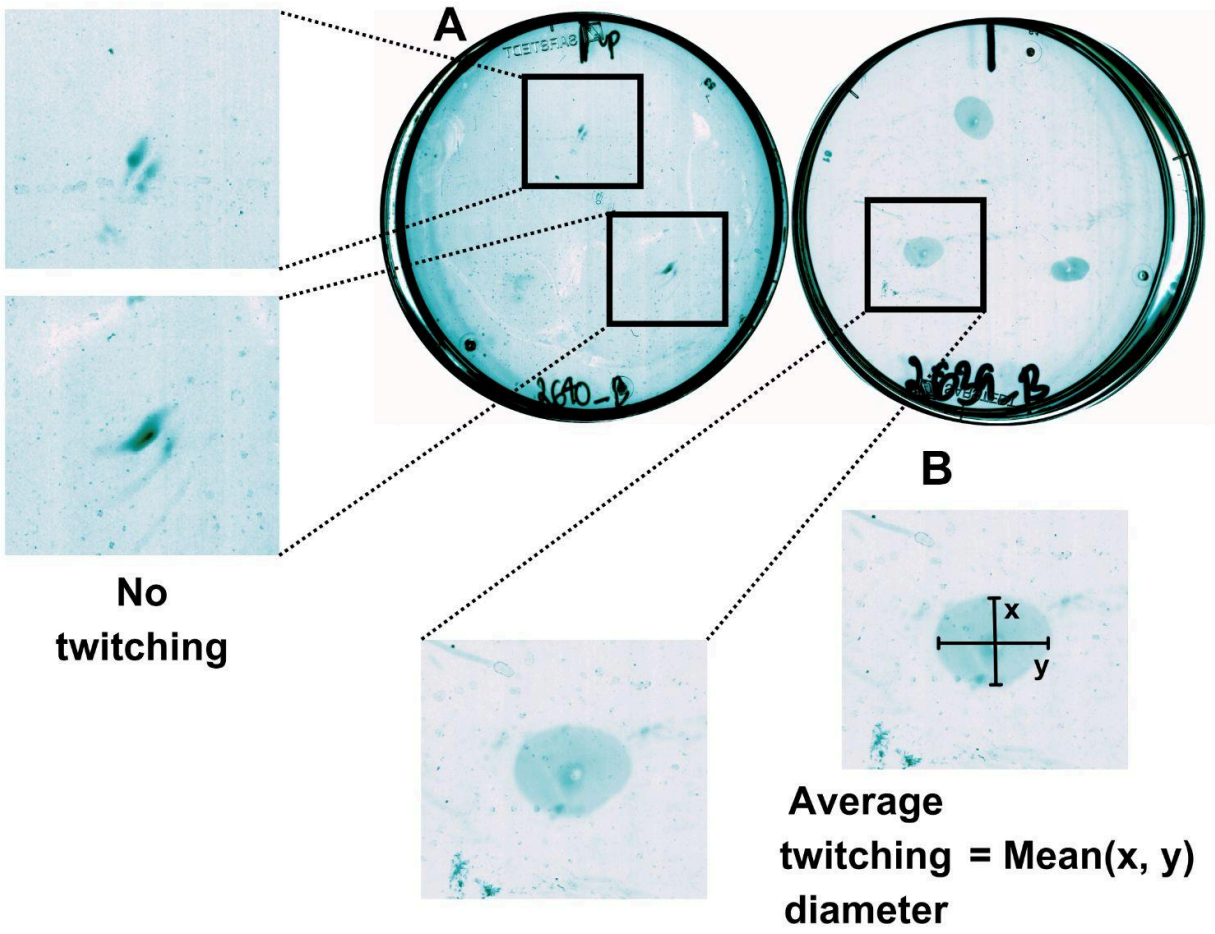

Figure 8 – Twitching Stab assay. The two plates are the positive and negative control strains. (**A**) The negative twitching control plate, zoomed in on two of the amorphous blobs that represent the stabbed bacteria. (**B**) The positive control plate, zoomed in on two of the colonies.

This was a fairly unpredictable assay, and sometimes only one or two of the three technical replicates would twitch, likely due to an issue with the stabbing technique. Sometimes none of them would twitch. In the case of only two twitching, the

non-twitching replicate would be disregarded, and the average of the two would be found. In the case of one or none, the entire plate would be disregarded.

2.2.6 *PaQa* reporter assay

This assay centres the *PaQa* plasmid – pUCP18_*pRpoD*-mKate_*pPaQa*-YFP.

The *PaQa* plasmid contains two fluorescent proteins under two promoters. The first is mKate under p*RpoD*, which is a strong constitutive promoter that controls the transcription of the primary sigma factor[36]. The second is YFP under *pPaQa*, which controls the *PaQa* operon[23]. The *PaQa* operon is one of the operons that get upregulated by the virulence factor regulator (Vfr), which is controlled by the intracellular cAMP in the cell, which in turn is dependent on surface attachment and the signalling thereof[23].

So under these conditions, mKate expression should be strong and relatively even across all cells, but YFP expression would depend on the surface-sensing signal that gets transmitted from TFP. By finding the ratio of the mKate and YFP signal from liquid and solid culture cells, this assay allows us to find out whether the signal is being transmitted, and how strongly. This forms the basis of a fairly robust sensor for intracellular cAMP[23].

The strains of interest were transformed with this plasmid using electroporation. 2-3 colonies were cultured for ~6 hours, and imaged under a 1% agarose PBS pad to confirm that the constitutive promoter was expressing mKate more-or-less evenly in all the cells (microscopy conditions for this were the same as the actual assay; they are mentioned in detail later in the protocol). Good candidates were cultured further and frozen for storage.

These were streaked out and cultured in 1mL of LB, with appropriate antibiotics. On the third day, 2mL of secondary culture was inoculated to a starting OD_{600} of 0.02, and each successive strain was inoculated with 0.5uL less primary culture that would be required for the same starting OD_{600}. These were allowed to grow for 3 hours at 37°C.

On the previous day, 1% agarose LB plates were poured – 5g of LB and 2g of agarose was dissolved in 200mL of distilled water, autoclaved, and allowed to cool in a 55°C water bath for 20 minutes. 28mL of the medium was poured into 6 petri plates, and allowed to dry, completely open, for exactly 30 minutes.

These were prewarmed an hour before use on the next day. 1% PBS agarose plates were poured about 30 minutes in advance, and pads would be stamped out.

At the 3h mark, the OD_{600} of the culture was measured, and the culture was diluted to 0.1. 1uL of the diluted culture was placed on a PBS pad and flipped onto a MatTek glass-bottomed dish.

100uL of the diluted culture was plated on a LB-agarose plate, spread lightly, and allowed to dry on its own. The plate was incubated at 37°C for 3h. The first PBS pad was imaged immediately – 3-10 images would be taken to achieve an approximate cell count of 100. The 3 hour time point was used because the *PaQa* signal peaks after 3 hours of surface incubation for the WT strain[26].

The imaging was done on a Nikon Widefield microscope at 100X magnification with an oil objective. Images were taken using the brightfield, YFP and RFP channels, with no binning.

After 3 hours, 1mL of LB was added to the plate, and shaken to rinse off the cells. The LB was pipetted over the plate repeatedly to wash the cells off, and the resulting sample was moved to a microcentrifuge tube. The OD_{600} of the sample was measured, and diluted down to 0.1. 1uL of the sample was placed on a PBS pad, which was flipped onto a dish, and imaged in the same manner as the first sample.

Image background was subtracted using ImageJ. The images were then segmented and the fluorescence was quantified using Bacstalk software [38], and code written by Marco Kühn, Chia-Ni Tsai, and other members of the lab. Segmentation was manually corrected. The ratio of yellow (YFP) to red (mKate) fluorescence was calculated for each cell, plotted on a scatter plot after being normalised to the WT, and the median found using Python.

The ImageJ, Matlab, and Python scripts used to accomplish this have been added to this Github page [39].

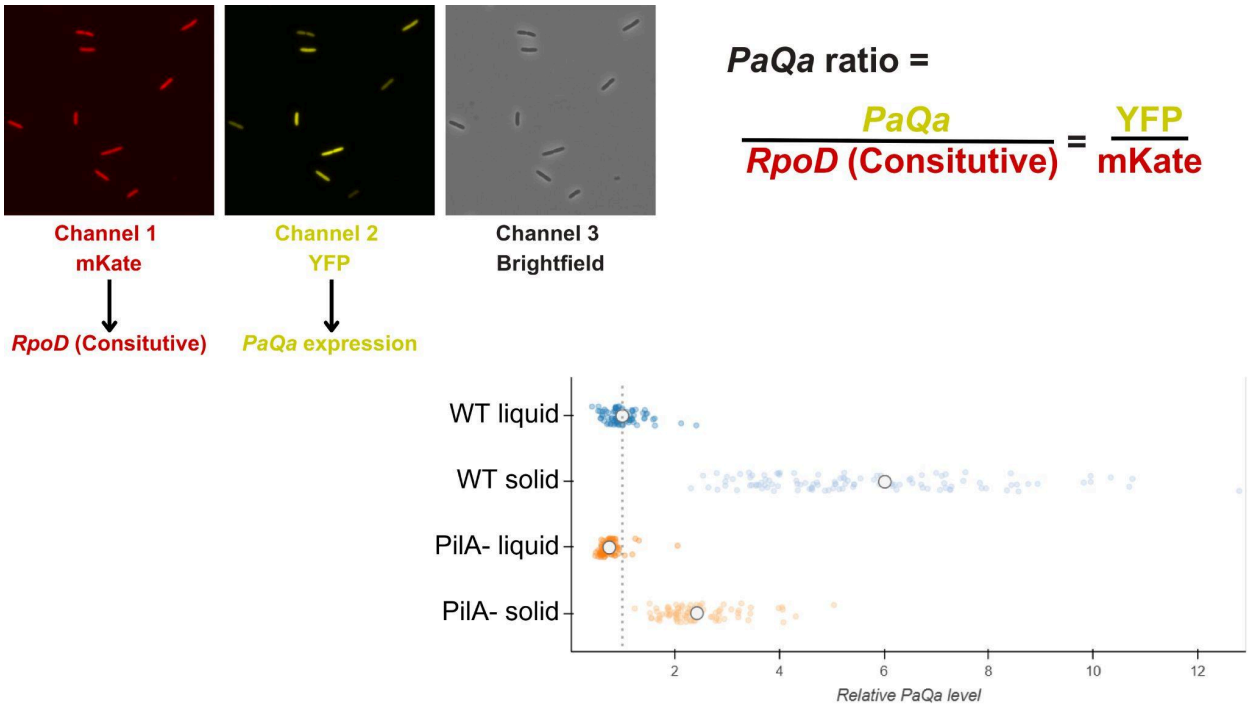

Figure 9 – The *PaQa* assay. The upper panel demonstrated the working of the assay, where the *PaQa* level is quantified by dividing YFP fluorescence with mKate. The lower panel shows the plotting of the data. The *PaQa* ratio of each data point (cell) is normalised against the reference strain, WT-liquid in this case, and added to a scatterplot. The median of each scatterplot is also plotted.

Results

3.1 Random mutagenesis

The following PilA mutants were generated with randomised primers –

G14 mutants	P22 mutants	
G14L	P22V	P22S
G14W	P22K	P22L
G14V	P22N	P22Y
G14A	P22G	P22C
G14Y	P22T	
G14N	P22I	

Table 3 – PilA helix-breaking mutants

These mutations were all conveyed into a PAO1 *ΔFliCΔPilA* mutant on the pJN105 plasmid, controlled by the WT *PilA* promoter. For all assays with the PilA mutants, positive and negative control strains refer to PAO1 *ΔFliCΔPilA*, containing the pJN105 plasmid, with and without the WT PilA gene respectively.

3.2 Luz19 infection time is affected by both pilus number and retraction

Given that Luz19 infects *P.aeruginosa* through the retraction of the pili, there are some factors that could play a role in a delay of infection. Conceivably, these are –

- Shorter/fewer pili – Both would mean fewer binding sites for the phage.
- Slower/less forceful retraction – May interfere with the process of infection.

To differentiate between these possibilities, some known strains were infected with the phage, with the aim of comparing the infection curves and gleaning any possible differences.

Strain	Cause for study
PAO1*ΔFliCΔPilB*	PilB is the extension motor of the Type IV pilus. Deleting it should yield a phenotype similar to deleting PilA.
PAO1*ΔFliCΔPilG*	The PilG deletion strain is known to have less pili [28] than the wildtype.
PAO1*ΔFliC PilA_A86C*	The PilA_A86C mutation is commonly done in TFP studies to label the pilus with maleimide. Unpublished data from Persat lab shows that it twitches slower and less frequently than the WT.
PAO1*ΔFliCΔPilU*	PilU is an accessory retraction motor that cannot replace PilT, but acts through it. The PilU deletion strain is known to exert a lower stall force than the WT[37].
PAO1*ΔFliC PilT_D160N*	The D160N mutation in PilT has been measured to exert a lower stall force than the WT retraction motor[37].

Table 4 – Test strains for phage infection

The two retraction force mutants show much higher susceptibility to the virus than the PilG- mutant. This is likely just an effect of relative magnitude – PilT_D160N and PilU- have an average stall force of 69% and 84% of WT[37]. Kühn et al (2021) estimated that the median PilG- bacterium has no pili at all, where the WT had about 5. Its average twitching diameter is about 25% of the WT.

There are no distinctive features in the curves themselves, so we conclude that the reason for a delay in infection cannot be deduced from the growth curve [Figure 10]. In addition, since the PilA mutations in section 3.1 were being introduced on a plasmid, further characterisation was done on the differences caused by the plasmid and the

antibiotic in the growth medium.

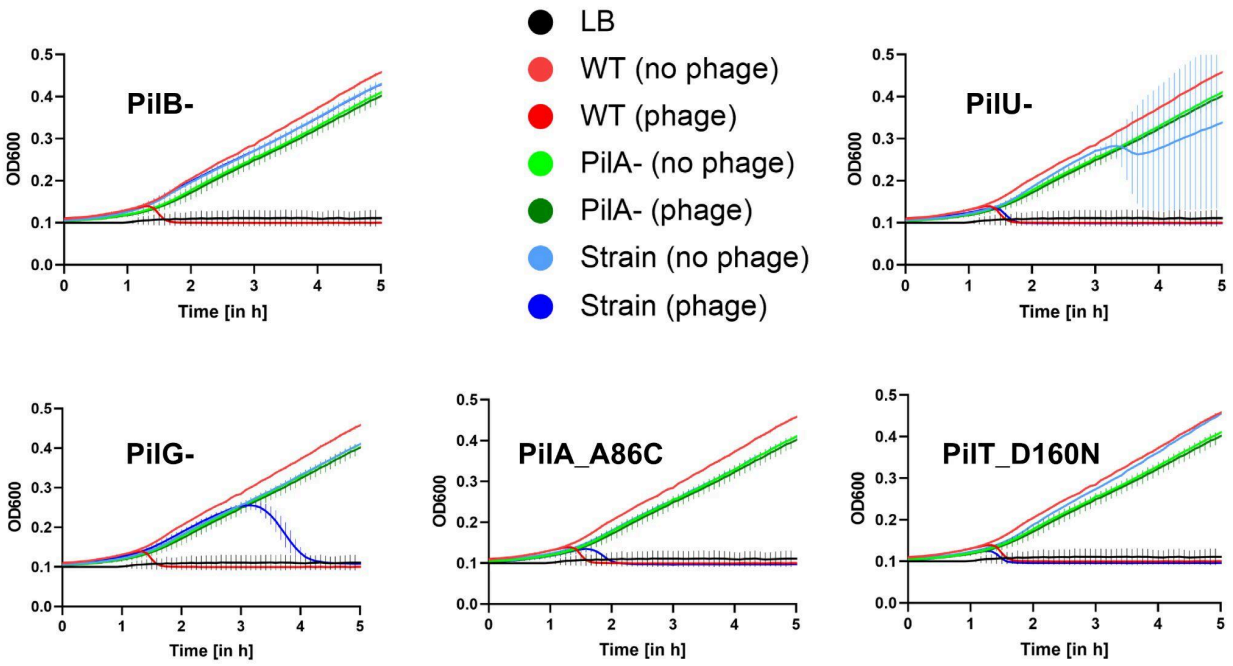

Figure 10 – Phage infection of Pil-Chp mutants. Curves represent the mean of three technical replicates, error bars represent the standard deviation. MOI for all infections is 10^{-4}.

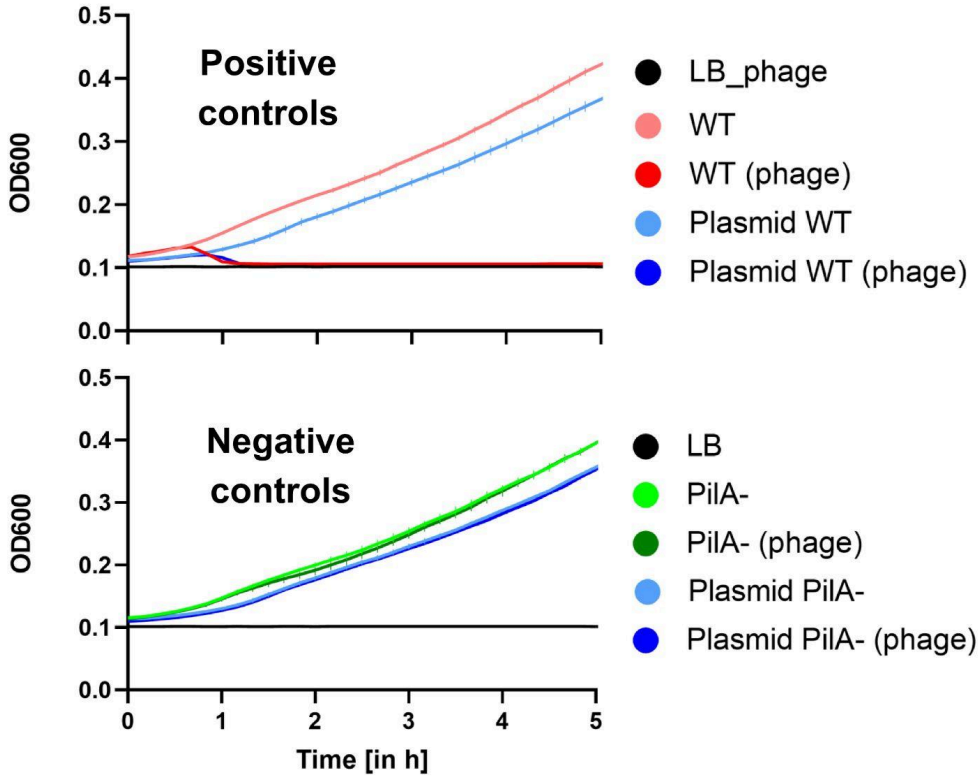

Figure 11 – Impact of the pJN105 plasmid on Luz19 infection. Curves represent the mean of three technical replicates, error bars represent the standard deviation. MOI for all infections is 10^{-4}.

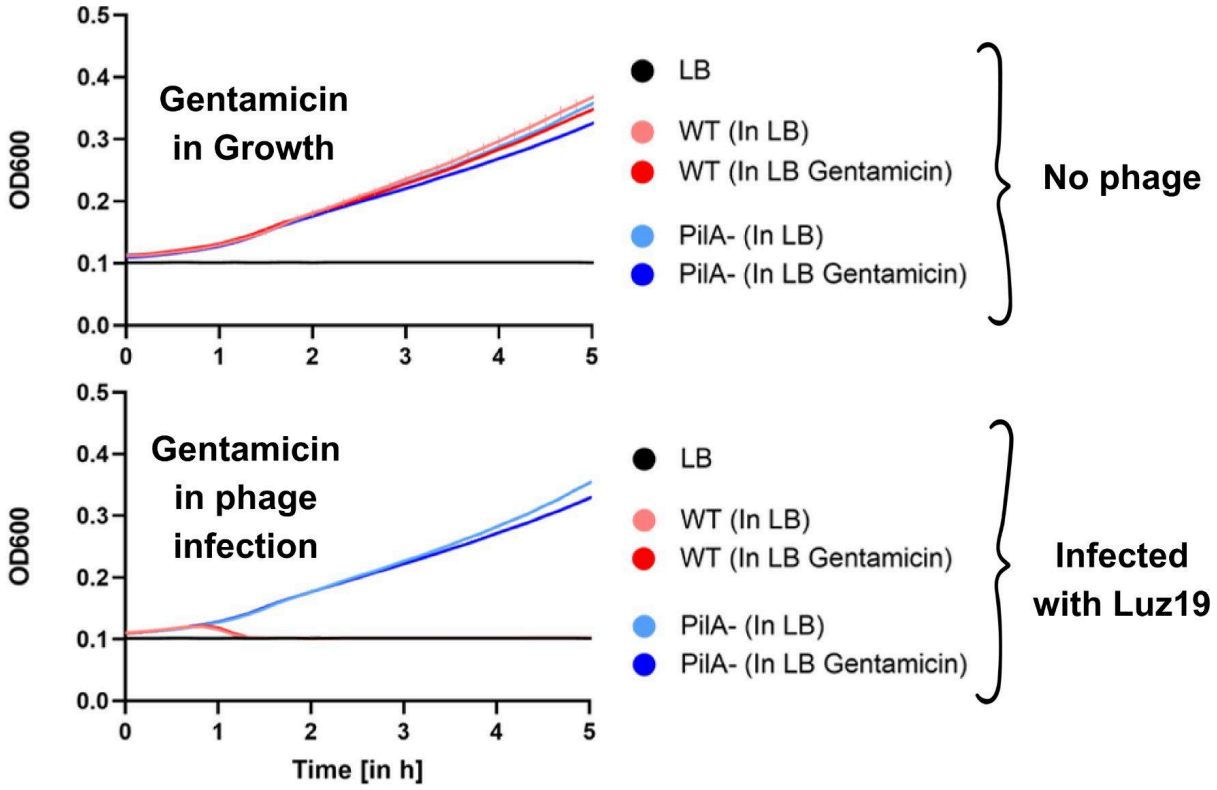

Figure 12 – Impact of gentamicin. Curves represent the mean of three technical replicates, error bars represent the standard deviation. MOI for all infections is 10^{-4}. Gentamicin concentration in this and in all experiments is 60 µg/mL.

Neither seem to make a considerable difference to the curve. Supplying the WT PilA gene on the pJN105 plasmid does seem to cause a small delay in the infection [Figure 11], in comparison to the *ΔFliC* strain, which contains PilA in its chromosome. It also seems to impact the growth of the strain to some extent, both in the case of the positive and negative control strain. This would suggest that the difference is the effect of maintaining the plasmid, and not due to a change in the copy number of the PilA gene.

Gentamicin causes a small reduction in growth in all cases, but notably, no change to the infection peak[Figure 12].

For all assays with the PilA mutants, positive and negative control strains refer to PAO1 *ΔFliC* containing the pJN105 plasmid, with and without the WT PilA gene respectively. They are all conducted with gentamicin in the medium.

3.3 Most PilA mutants can form functioning pili

The strains were infected with Luz19 to understand whether pili were present and functional.

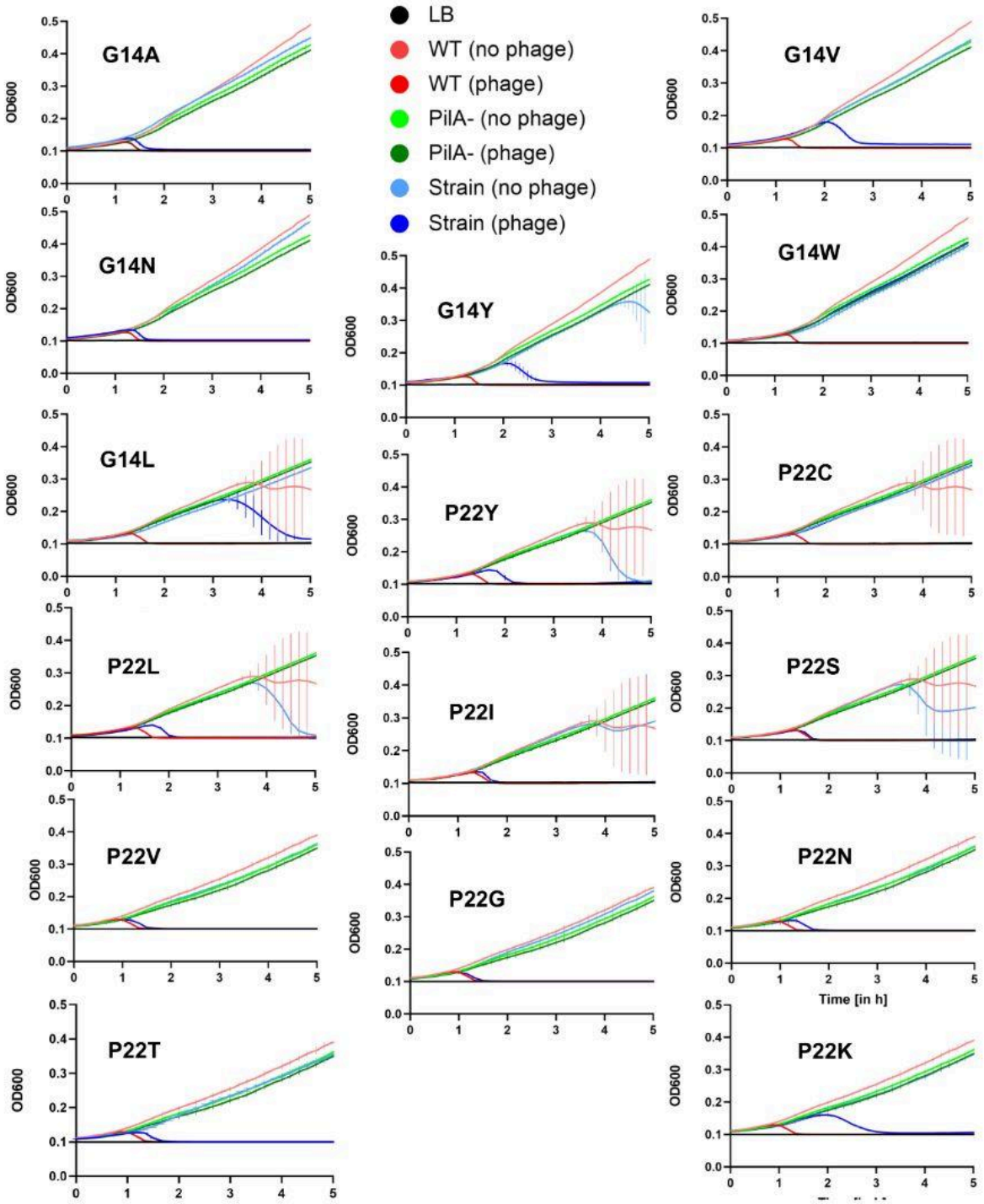

Figure 13 – Phage infection of G14 and P22 mutants. Each curve represents the mean and standard deviation of three technical replicates. The MOI for all infections was 10^{-4}.

Growth curves measurements were done for each strain in triplicate – three technical replicates each of three biological replicates. One representative biological replicate is shown for each strain in Figure 13.

The delay in the peak was measured against the positive control (FliC- PilA- pJN105-WT-PilA) for each strain and plotted.

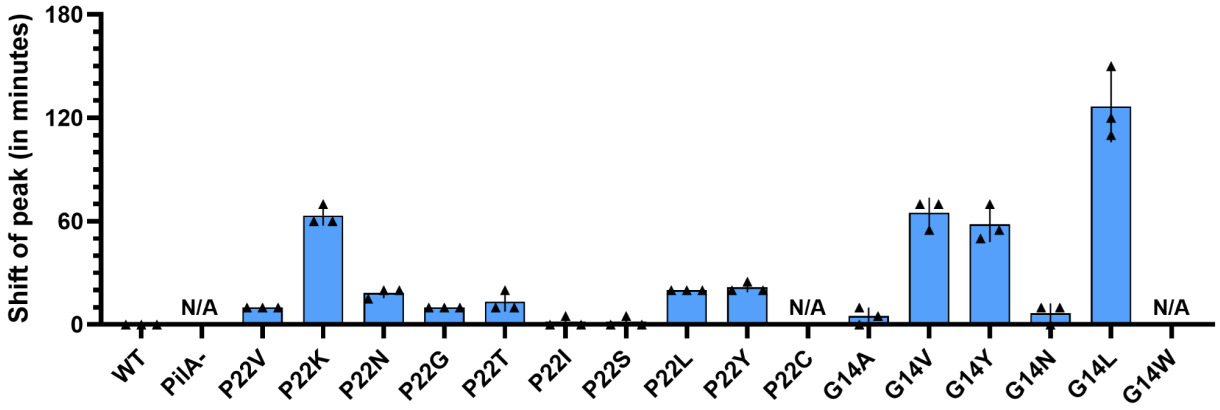

Figure 14 – Delay in infection peak for PilA mutants. The value that is being plotted here is (time of $peak_{mutant}$ - time of $peak_{+ve\text{-}control}$). Each data point represents a biological replicate. Absence of a bar means there was no discernible peak at all within 10 hours of the start of the assay i.e. the mutant is functionally immune to the virus (marked by N/A). MOI for all infections was 10^{-4}.

As the infection demonstrates, most mutants are able to form functioning pili. P22C and G14W are the only single mutants that show complete immunity to the virus, likely indicating that they cannot form pili at all.

Regardless, this does indicate that neither of the pilus-breaking residues are irreplaceable to the assembly and function of the Type IV pilus.

Small and relatively non-polar amino acids seem to have the lowest impact on the infection. This is unsurprising – the core of the pilus is a narrow and hydrophobic region, and a large or charged residue would likely disturb the interior of the protein, leading to

issues with assembly, or with the stability of the pilus.

Following this, phase contrast microscopy was used to understand how well these mutants could actually twitch, and how well the results of the infection assay translated to real motility.

3.4 Most PilA mutants show twitching motility

A drop of bacterial culture was incubated beneath an agar pad for 2 hours to allow the strains to grow pili and transition into surface-attached cultures. These were then imaged for 5 minutes continuously, with images taken every 5 seconds.

Table 4 contains cropped stills from the video – 4 images of the same frame 20s apart.

Time-lapse post-incubation (0s, 20s, 40s, 60s) (36✖36uM)			
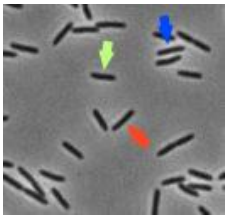	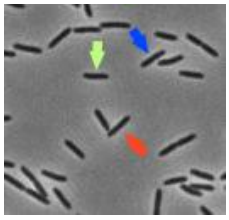	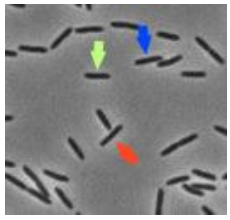	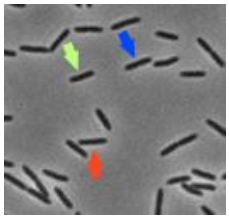
A - Positive twitching control			
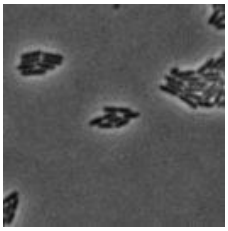	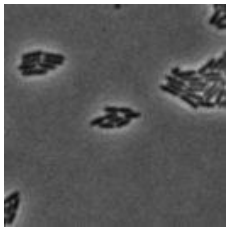	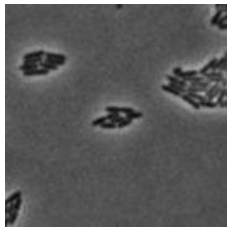	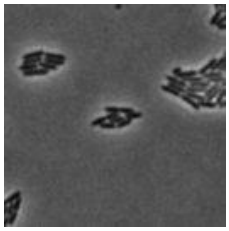
B - Negative twitching control			

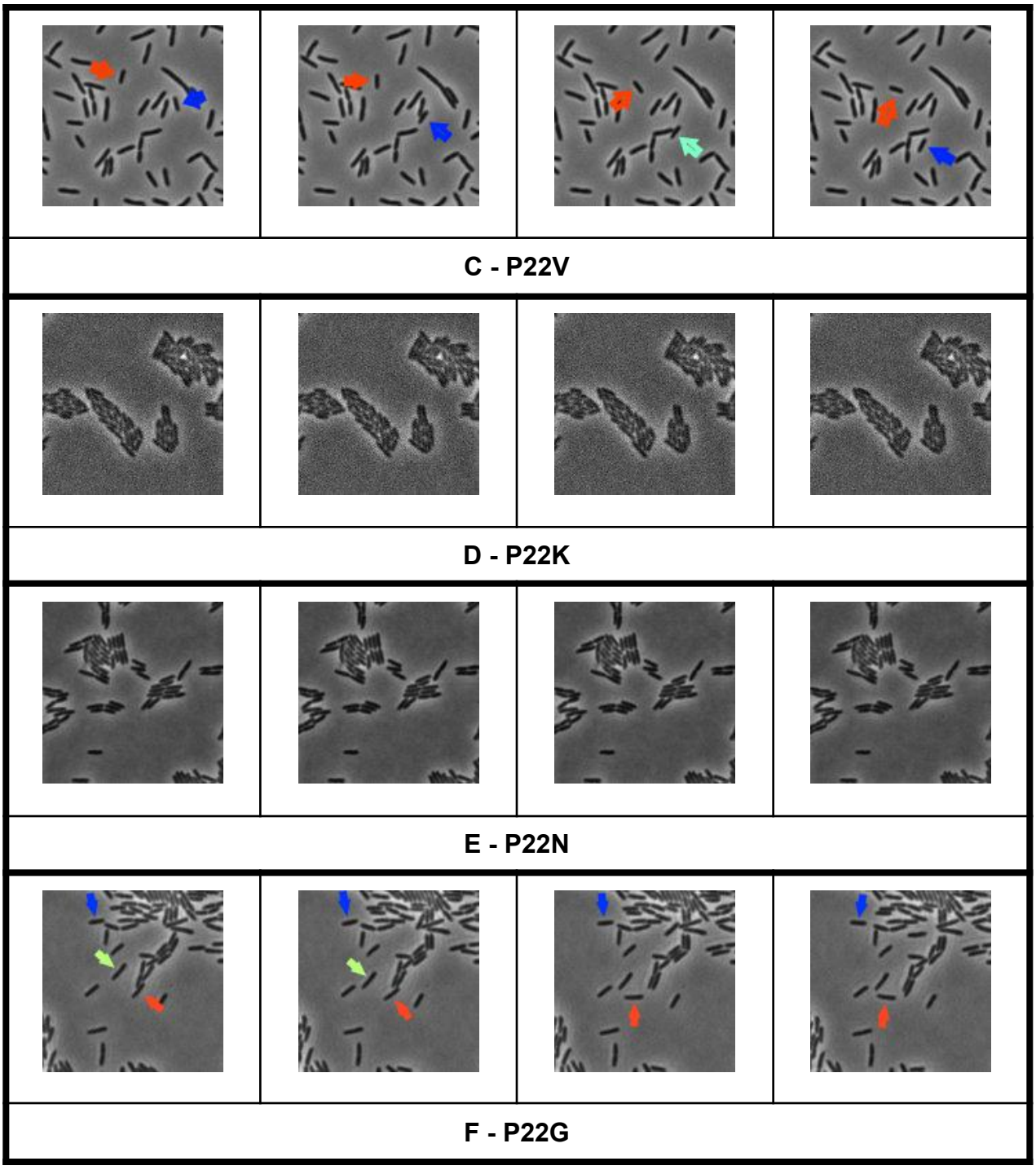
C - P22V
D - P22K
E - P22N
F - P22G

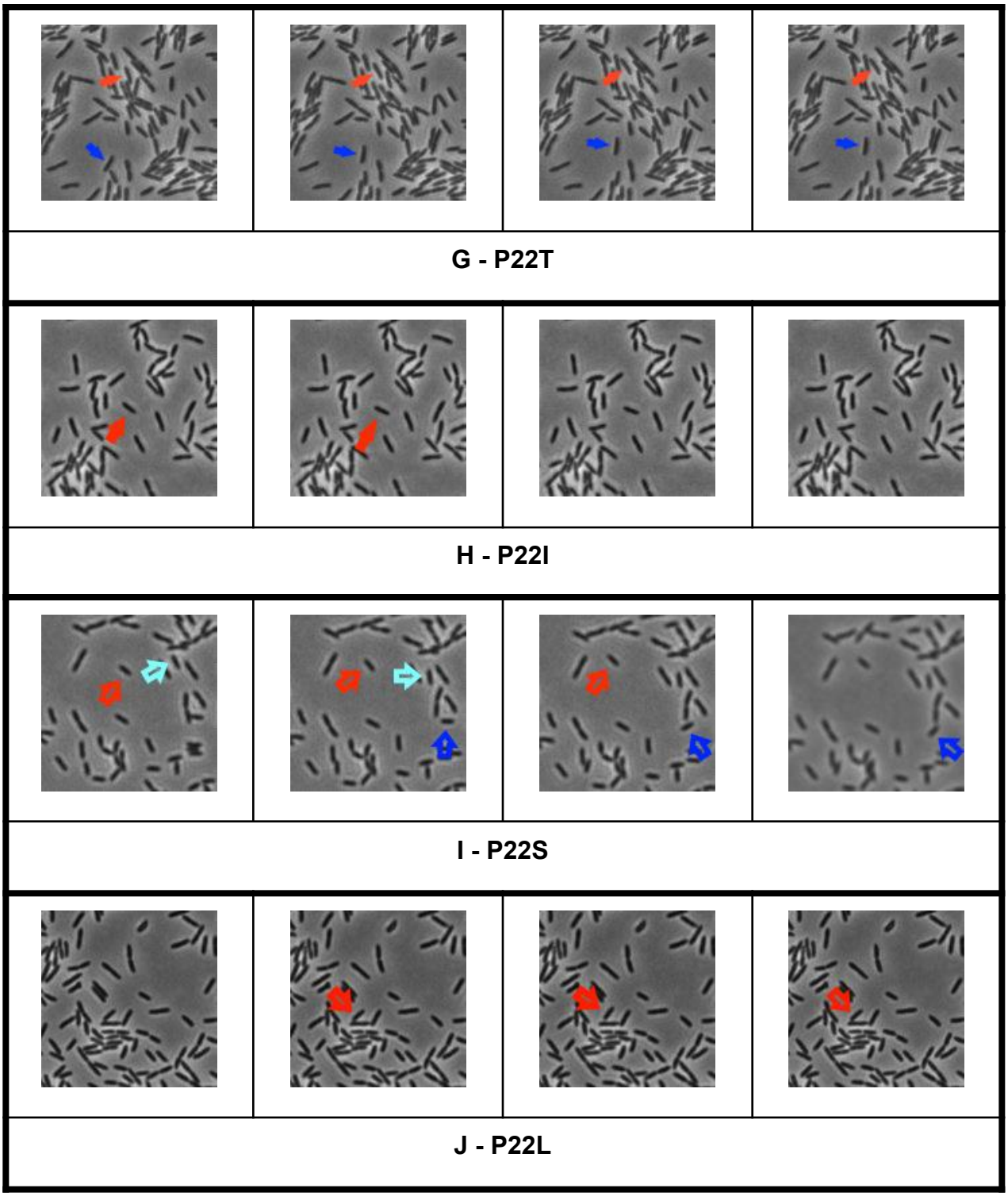

G - P22T

H - P22I

I - P22S

J - P22L

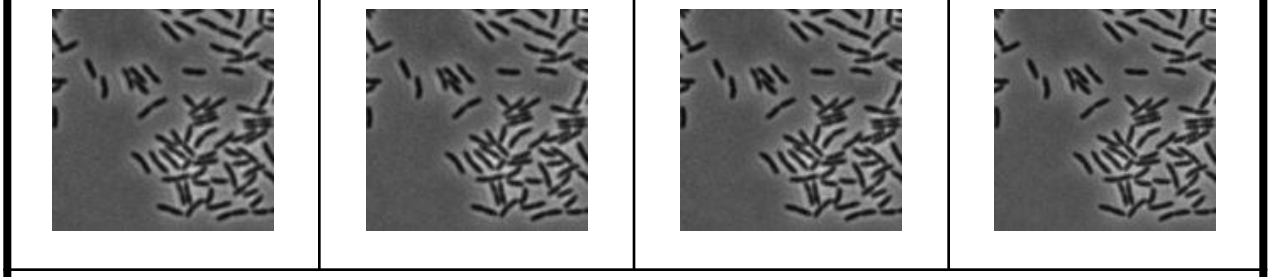

K - P22C

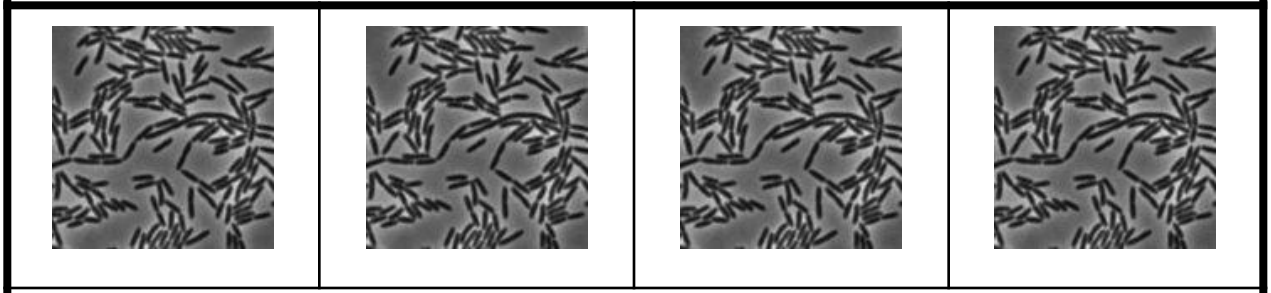

L - P22Y

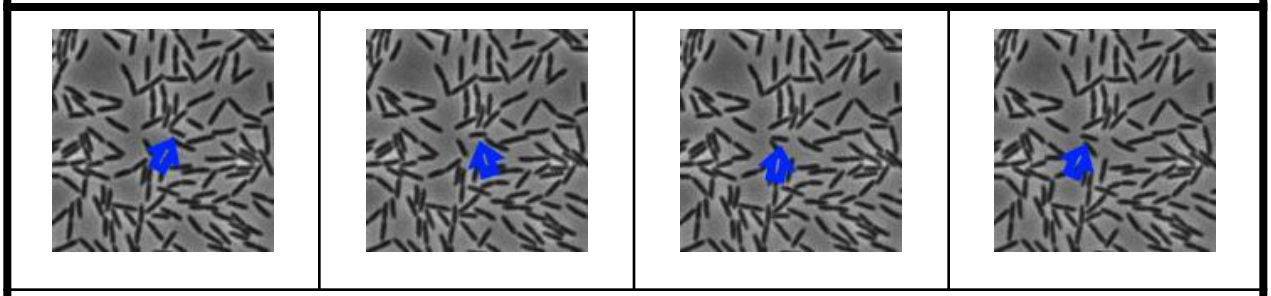

M - G14A

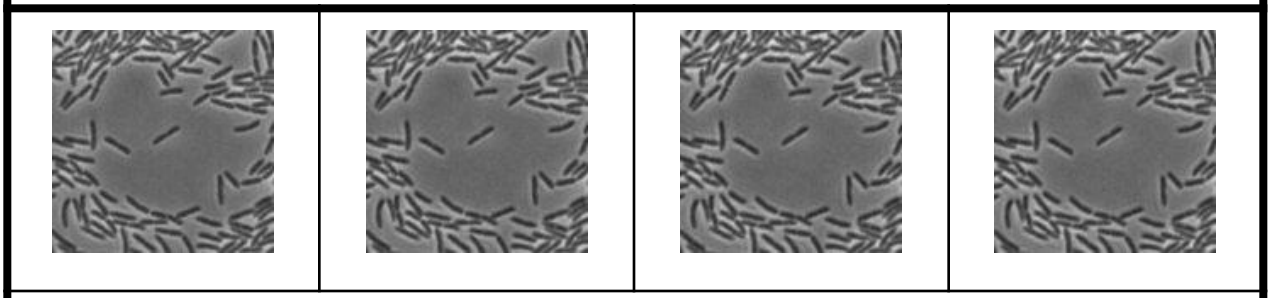

N - G14V

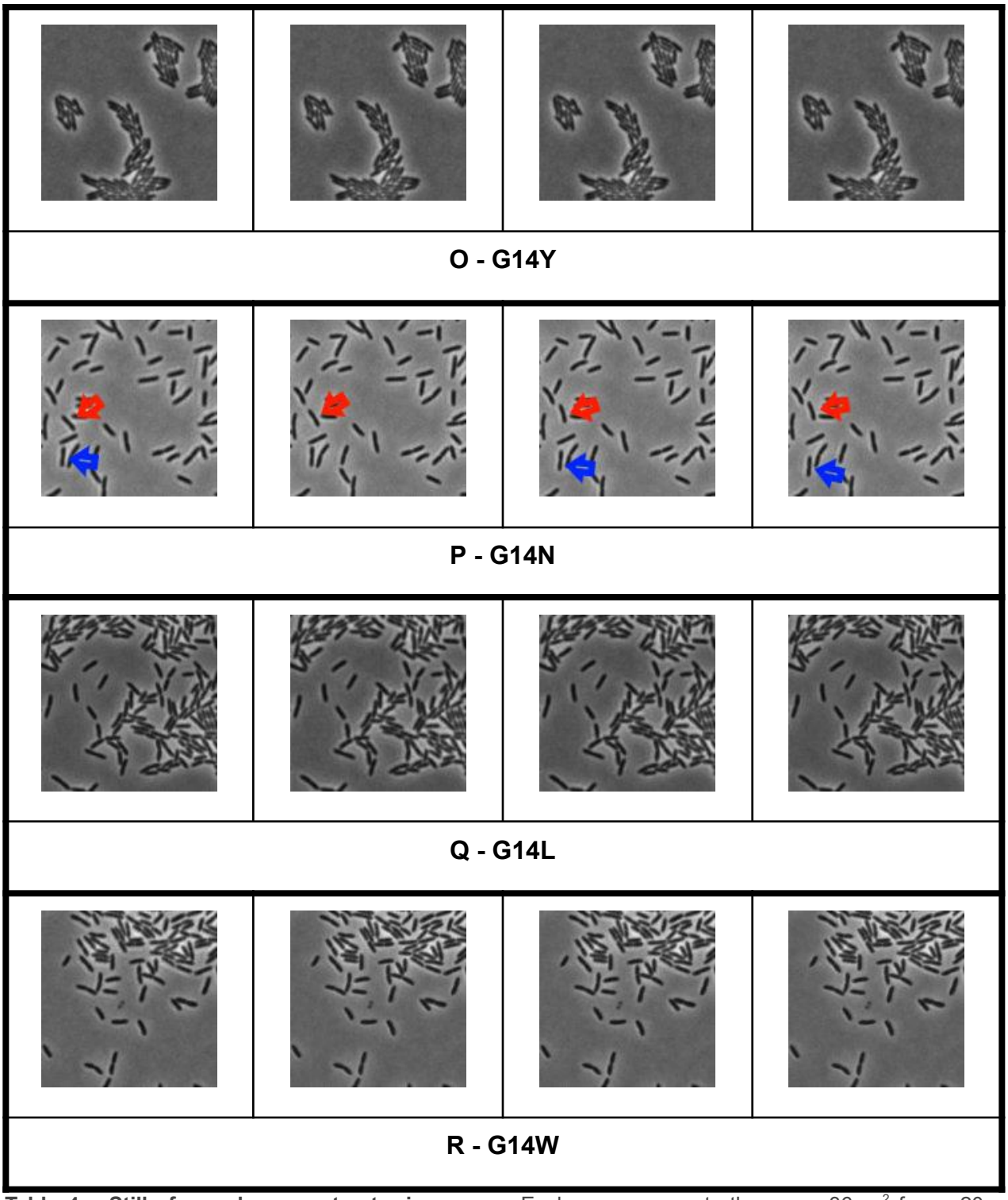

Table 4 – Stills from phase contrast microscopy. Each row represents the same 36μm^2 frame 20s apart. Moving cells are marked by colored arrows.

It is evident from this that most of the mutants are also able to twitch to some extent, unless the residue is mutated to a very large or charged amino acid.

As a rough quantification, about a 100 cells from 3-4 frames were selected and observed visually over the full five minute period – any independent movement was noted. Independent movement here refers to any movement of a cell that could not conceivably be ascribed to movement caused by the growth of other cells or pushing by other cells. The results are tabulated in Table 5, in decreasing order of twitching frequency.

As seen in Figure 7, twitching and non-twitching mutants appear distinct when imaged – twitching phenotypes are spread out, and non-twitching phenotypes are clumped together. So while the microscopy was not able to catch any movement, some strains, like P22C, have single cells that lie apart from the large clumps of bacteria. This would suggest that they do twitch to some small extent; longer periods of monitoring may help to remedy this, to spot if the cells twitch slower or upon greater levels of crowding.
The protocol here evidently has some limitations – the sample is only recorded for five minutes at a single time point of 2 hours. PilA mutations are very likely to create unstable pili, so it's entirely possible that the movement of these mutants is slow and jerky, caused by reduced pilus numbers, increased pilus breakage and so on.

To partially overcome the limitations, the twitching stab assay was done on the strains. The results have been graphed in Figure 15 and added to Table 5.

Mutant	No. of cells that showed independent movement (**A**)	No.of cells observed (**B**)	**A/B** expressed as a % of the WT (**C**)	Relative twitching diameter
WT	93	102	100	1
G14N	80	108	81.2	0.91
P22S	58	103	61.8	0.72

P22V	54	119	49.8	0.70
P22G	53	118	49.3	0.67
G14A	32	105	33.4	0.39
P22I	30	100	32.9	0.64
P22T	19	145	14.4	0.42
P22L	8	144	6.1	0.45
P22Y	1	110	1	0.40
G14L	1	167	0.7	0.50
P22C	0	139	0	0.4
P22K	0	120	0	0.43
P22N	0	102	0	0.53
G14V	0	130	0	0.56
G14W	0	124	0	0.23
G14Y	0	120	0	0.20
PilA-	0	110	0	0.11

Table 5 – Twitching quantification. **A** represents the number of cells that showed independent movement in any of the 300 seconds of recording, and **B** represents the total number of cells observed. **C** refers to $(A/B)_{strain}/(A/B)_{WT}$. Clear twitching phenotypes are marked by green cells.

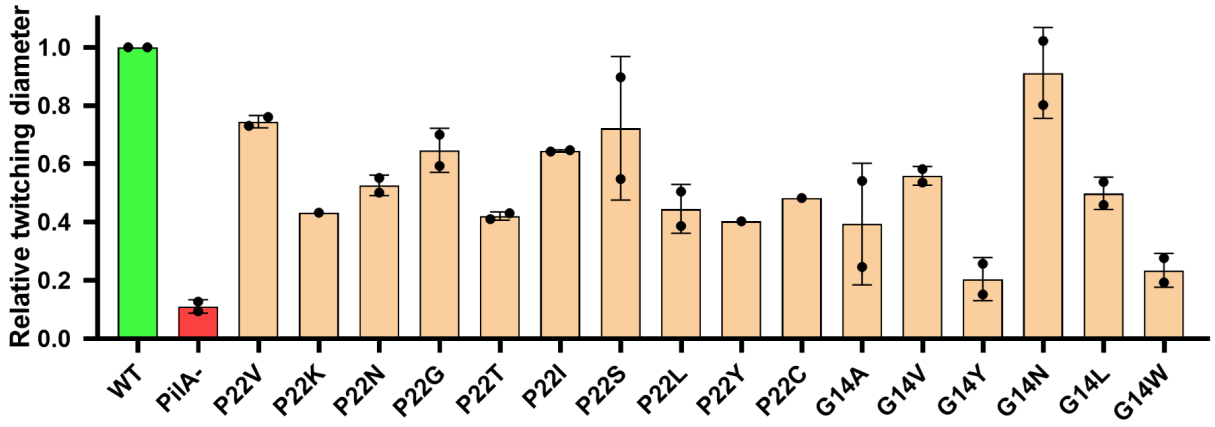

Figure 15 – Average Twitching diameter of PilA mutants. Each bar represents one (P22K, P22Y, P22C) or two bio-replicates. Each bio-replicate is the average of three technical replicates.

As suspected, some of the non-moving mutants did show a clear twitching phenotype under the conditions of the stab assay.

The two twitching assays disagree drastically over some strains – G14V and P22N, for instance, do not twitch independently at all under the microscope, but show twitching diameters about as high or higher than strains like P22L and P22T, which do visibly twitch. It is not clear why this happens, but it's possible that the mutants could have distinct defects of assembly and stability. The short incubation period (2 hours) prior to the microscopy may not be allowing these mutants to form pili, while 18 hours gives them enough time to do so. P22L and P22T may have pili that are more prone to breakage, leading to the overall twitching defect, but still assemble comparatively faster, allowing a small percentage of the cells to be moving when observed under the microscope. This could be clarified with labelling of the pilus for direct imaging – to derive assembly times and average length.

The infection assay seems quite effective at predicting whether the cell can twitch. The only strain it was not able to correctly predict was P22C, which does not get infected at all. G14Y is the only strain that does not twitch at all despite infection.

Our understanding that small and non-polar residues can effectively replace the helix-breaking residues is illustrated quite clearly by the microscopy.

P22V twitches more than P22L and P22I. P22S twitches more than P22T. The really large mutations, tyrosine and tryptophan, do not twitch at all. Size evidently has an unfavorable effect, implying that the fault caused by the non-polar mutations, in some part, is structural.

P22T twitches less than P22V, and less than P22I, so the polarity of the hydroxyl group makes a difference. P22S twitches similarly to P22V, however, so it cannot be said to be

a greater factor than size. It is certainly more complicated than size, because G14N is the only mutation that twitches at near-WT levels.

G14 generally seems more intolerant of mutations that P22 seems to absorb quite well. P22L and P22V can twitch, while G14L and G14V cannot. Neither P22Y or G14Y can twitch, but the latter shows a much greater delay when infected with Luz19. It may be that the G14 has a smaller pocket to fit in the pilus filament to fit in compared to P22 – making it much more intolerant of larger residues.

G14N represents a complication here – it contradicts most of what has been said so far in this section. G14N is the most motile of the whole suite of mutants, by a significant margin.
Studying the structure of the TFP[31] shows us that Lysine145 of the outer pilus sits quite close to G14. It's possible that the mutation allows for hydrogen-bonding between the two residues, conferring some unexpected stability on the mutated pilus.
G14N is also the only polar mutation made at that residue – further mutations would help clarify whether charged residues are not as detrimental at G14 as they are at P22. Mutations of K145 and other neighbouring residues could also help with understanding why G14N is so stable and motile.

It seemed at this point that small, uncharged residues were the most successful at replacing the two helix-breaking residues. With this in mind, double mutants G14A-P22A and G14V-P22V were designed and cloned.

3.5 Double mutants do not produce functional pili

Upon testing, however, the double-alanine and double-valine mutants showed phenotypes close to PilA-.
They showed complete immunity to Luz19 infection; microscopy and the stab assay revealed that they do not twitch at all, as seen in Figure 16.

From this, we can understand that whatever flexibility is lost by a single mutation may be tolerable, but double mutants of even small amino acids completely disrupt the assembly process. All four of the component mutants can twitch, but the combination does not.

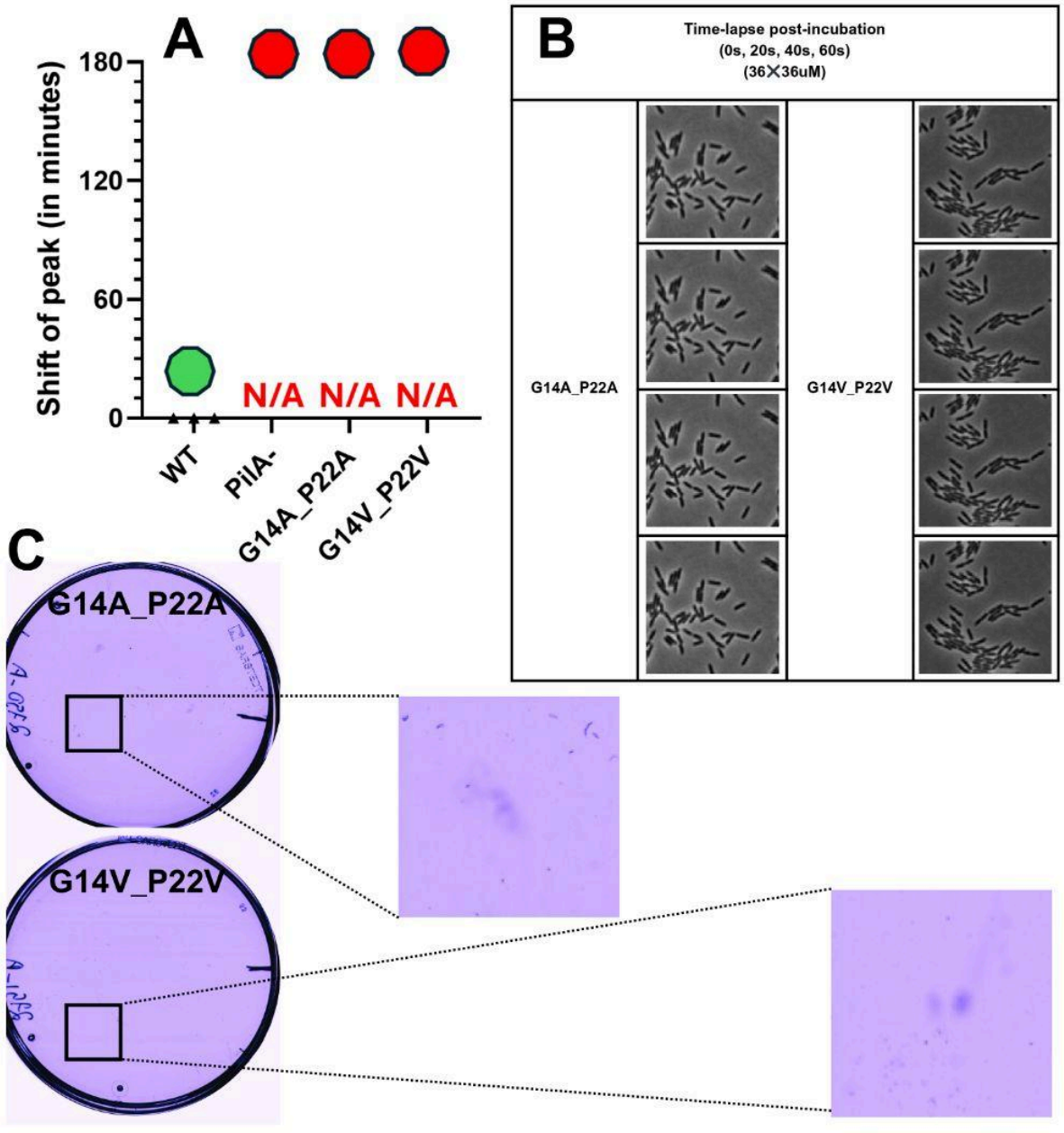

Figure 16 – Double mutants do not form functional pili. (**A**) Phage infection (**B**) Stills from phase contrast microscopy (**C**) Twitching stab assay

3.6 Twitching and non-twitching mutants show distinct *PaQa* profiles

The *PaQa* reporter assay was done on some of these constituent mutants, and the G14A_P22A and G14V_P22V double mutants – to see if twitching ability was correlated with downstream signalling, and if the melted region played a part in it.

G14Y was also tested because it was observed to have a lower growth rate during experimentation, and because it is one of the only two single mutants that does not show twitching in the stab assay.

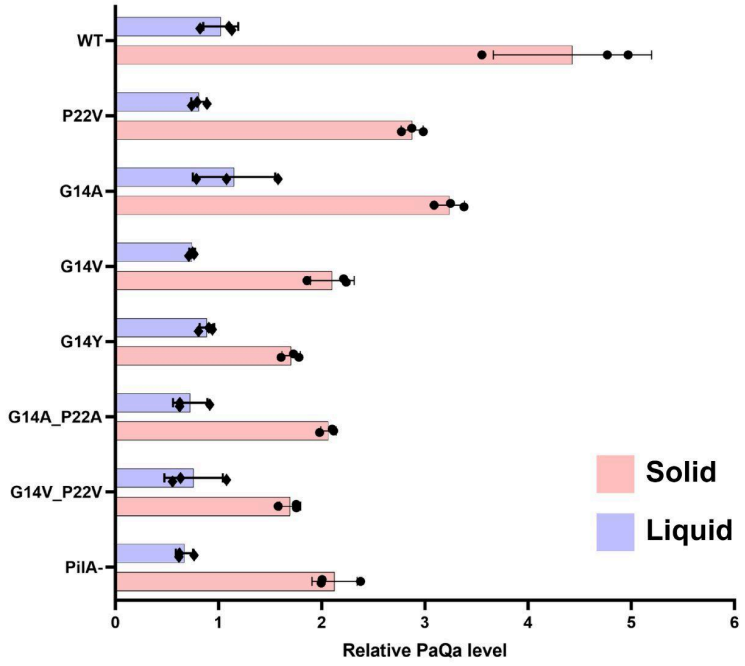

Figure 17 – *PaQa* ratio of PilA mutants. Bar graph of the *PaQa* values, normalised to the WT liquid level. Each strain represents three bio-replicates, and each bio-replicate represents the median of some 100-odd cells.

None of the mutants are comparable to the WT, but P22V and G14A are both significantly higher than the rest of the mutants.

G14V, despite twitching in the stab assay, shows a similar level of activation as the three mutants that do not twitch at all. This is strange, but the stab assay is analysed after 18 hours of incubation. From microscopy, we do know that G14V does not show twitching at all after 2 hours of incubation on a solid surface. The *PaQa* assay is conducted after 3 hours of incubation, so it's entirely possible that the strain may show both twitching and *PaQa* activation after a longer period of incubation.

It is evident that the activation phenotype follows from the twitching phenotype observed under microscopy. While it cannot be stated for certain without further study, we can hypothesise that the two defects likely have the same cause, with assembly and/or stability. That is to say, the activation defect is caused by the twitching defect, and not by the mutation itself, suggesting that the melted region has no involvement in signalling.

Conclusion and Future directions

It's clear that the two helix-breaking residues are important to the functioning of the pilus, but also that they are not irreplaceable.

The core of the pilus is a narrow and hydrophobic region, so it is not surprising that mutations to large or very charged residues are detrimental to the assembly and stability of the pilus filament. None of the tested mutations allow for full WT levels of motility, but several of them retain Intermediate levels.

The double mutants are both completely unable to twitch and have a nearly identical *PaQa* profile as the negative control indicating that the dysfunction causing by single mutations do compound. The cloning of G14N double mutants was attempted and abandoned over the course of the project – given that G14 seems so intolerant of non-polar residues, it may be interesting to see whether a G14N_P22X double mutant is able to form working pili.

Regardless, it seems that one of two things must be true –

- G14 and P22 are not the cause of the melted region. This may be true in the absolute sense – that neither of them are at all responsible. More likely is that they each contribute without being solely responsible for it. Mutating one of them lessens the flexibility of the region, or perhaps creates some partial structure in place of it, but only by mutating both of them can it be fully disrupted.
- The melted region is not essential to the functioning of the pilus. The mutations prevent the "melting", but this does not lead to any dysfunction – the differences caused by the mutations don't have anything to do with it. Perhaps the residues contribute independently to protein-protein contact in assembly and retraction and sensing, and the changes measured in the mutants are simply a result of that.

Structural analysis of the mutated TFP would resolve this, both of the relaxed pilus and one under tensile force, to understand whether the melted region has been eliminated by mutation/s, and if the “stretchability” of the pilus has been compromised. The latter could also be studied by physically pulling on the TFP and comparing the force-response curve to that of the WT.
Koch et al. (2022) posited that the melted region may be a key component in the cell's response to surface stiffness. Testing the *PaQa* response of these mutants to a range of stiffnesses may also go toward experimentally proving their hypothesis.

The results of the *PaQa* assay show a close association of the motility of the mutants to the downstream signalling, suggesting that whatever the structural role of the residues or the region as a whole, it does not play a role in signalling.
As a strong caveat to this hypothesis, it should be stated that *PaQa* signalling was only tested for non-polar mutants, when glycine and proline are both also non-polar. It’s possible signalling does take place at these residues, and the mutations simply did not disrupt them. Testing motile, polar mutants like P22S and G14N would further our understanding of this.

To conclude, the melted region of the TFP monomer is a fascinating structural feature of the system. Its role is still largely unknown, but the residues thought responsible for creating it have proved much more mutable than previously thought.

References

[1] - Gessard, Carle. Classics in infectious diseases. “On the blue and green coloration that appears on bandages.” By Carle Gessard (1850-1925). Rev Infect Dis 1984;6Suppl 3:S775-6

[2] - Moore, NM, Flaws, M. “Introduction: Pseudomonas aeruginosa.” *Clin Lab Sci* 24:41–42. 2011, doi: 10.29074/ascls.24.1.41

[3] - Arai, Hiroyuki. “Regulation and Function of Versatile Aerobic and Anaerobic Respiratory Metabolism in Pseudomonas aeruginosa.” *Frontiers in microbiology* vol. 2 103. 5 May. 2011, doi:10.3389/fmicb.2011.00103

[4] - Stover, C., Pham, X., Erwin, A. *et al.* Complete genome sequence of *Pseudomonas aeruginosa* PAO1, an opportunistic pathogen. *Nature* 406, 959–964 (2000), doi:10.1038/35023079

[5] - WHO Bacterial Priority Pathogens List, 2024: bacterial pathogens of public health importance to guide research, development and strategies to prevent and control antimicrobial resistance. Geneva: World Health Organization; 2024.

[6] - Miller, W.R., Arias, C.A. ESKAPE pathogens: antimicrobial resistance, epidemiology, clinical impact and therapeutics. *Nat Rev Microbiol* 22, 598–616 (2024), doi:10.1038/s41579-024-01054-w

[7] - Liu, H.Y., Prentice, E.L. & Webber, M.A. Mechanisms of antimicrobial resistance in biofilms. *npj Antimicrob Resist* 2, 27 (2024), doi:10.1038/s44259-024-00046-3

[8] - Parrilli, E., Tutino, M.L. & Marino, G. Biofilm as an adaptation strategy to extreme conditions. *Rend. Fis. Acc. Lincei* 33, 527–536 (2022), doi:10.1007/s12210-022-01083-8

[9] - Costerton, J W et al. “How bacteria stick.” *Scientific American* vol. 238,1 (1978): 86-95. doi:10.1038/scientificamerican0178-86

[10] - Siryaporn, Albert et al. “Surface attachment induces Pseudomonas aeruginosa virulence.” Proceedings of the National Academy of Sciences of the United States of

America vol. 111,47 (2014): 16860-5. doi:10.1073/pnas.1415712111

[11] - Laventie, Benoît-Joseph, and Urs Jenal. “Surface Sensing and Adaptation in Bacteria.” *Annual review of microbiology* vol. 74 (2020): 735-760. doi:10.1146/annurev-micro-012120-063427

[12] - Monds RD, Newell PD, Gross RH, O’Toole GA. 2007. Phosphate-dependent modulation of c-di-GMP levels regulates Pseudomonas fluorescens Pf0–1 biofilm formation by controlling secretion of the adhesin LapA. Mol. Microbiol. 63(3):656–79

[13] - Ponsonnet, L., Boureanu, M., Jaffrezic, N., Othmane, A., Dorel, C., & Lejeune, P. (2008). *Local pH variation as an initial step in bacterial surface-sensing and biofilm formation. Materials Science and Engineering: C, 28(5-6), 896–900.* doi:10.1016/j.msec.2007.10.031

[14] - Ellison CK, Kan J, Dillard RS, Kysela DT, Ducret A, Berne C, Hampton CM, Ke Z, Wright ER, Biais N, Dalia AB, Brun YV. 2017. Obstruction of pilus retraction stimulates bacterial surface sensing. *Science* 358:535–538.

[15] - Schniederberend M, Williams JF, Shine E, Shen C, Jain R, Emonet T, Kazmierczak BI. 2019. Modulation of flagellar rotation in surface-attached bacteria: a pathway for rapid surface-sensing after flagellar attachment. *PLoS Pathog* 15:e1008149.

[16] - O'Toole, George A, and Gerard Cl Wong. “Sensational biofilms: surface sensing in bacteria.” *Current opinion in microbiology* vol. 30 (2016): 139-146. doi:10.1016/j.mib.2016.02.004

[17] - Graham, Katherine J, and Lori L Burrows. “More than a feeling: microscopy approaches to understanding surface-sensing mechanisms.” *Journal of bacteriology*, vol. 203,6 e00492-20. 19 Oct. 2020, doi:10.1128/JB.00492-20

[18] - Kilmury, S. L. N., & Burrows, L. L. Type IV pilins regulate their own expression via direct intramembrane interactions with the sensor kinase PilS. *Proceedings of the National Academy of Sciences, 113(21), 6017–6022.* (2016) doi:10.1073/pnas.1512947113

[19] - M.D. Koch, C. Fei, N.S. Wingreen, J.W. Shaevitz, & Z. Gitai, Competitive binding

of independent extension and retraction motors explains the quantitative dynamics of type IV pili, *Proc. Natl. Acad. Sci. U.S.A.* 118 (8) e2014926118, (2021) doi:10.1073/pnas.2014926118

[20] - Kuchma, Sherry L, and George A O'Toole. “Surface-Induced cAMP Signaling Requires Multiple Features of the Pseudomonas aeruginosa Type IV Pili.” *Journal of bacteriology* vol. 204,10 (2022): e0018622. doi:10.1128/jb.00186-22

[21] - Gold, Vicki, and Mikhail Kudryashev. “Recent progress in structure and dynamics of dual-membrane-spanning bacterial nanomachines.” *Current opinion in structural biology* vol. 39 (2016): 1-7. doi:10.1016/j.sbi.2016.03.001

[22] - Maier, Berenike et al. “Single pilus motor forces exceed 100 pN.” *Proceedings of the National Academy of Sciences of the United States of America* vol. 99,25 (2002): 16012-7. doi:10.1073/pnas.242523299

[23] - Persat, Alexandre et al. “Type IV pili mechanochemically regulate virulence factors in Pseudomonas aeruginosa.” *Proceedings of the National Academy of Sciences of the United States of America* vol. 112,24 (2015): 7563-8. doi:10.1073/pnas.1502025112

[24] - Salah Ud-Din, A. I. M., & Roujeinikova, A. (2017). *Methyl-accepting chemotaxis proteins: a core sensing element in prokaryotes and archaea. Cellular and Molecular Life Sciences, 74(18), 3293–3303.* doi:10.1007/s00018-017-2514-0

[25] - Biais, Nicolas et al. “Force-dependent polymorphism in type IV pili reveals hidden epitopes.” *Proceedings of the National Academy of Sciences of the United States of America* vol. 107,25 (2010): 11358-63. doi:10.1073/pnas.0911328107

[26] - Koch, Matthias D et al. “*Pseudomonas aeruginosa* distinguishes surfaces by stiffness using retraction of type IV pili.” *Proceedings of the National Academy of Sciences of the United States of America* vol. 119,20 (2022): e2119434119. doi:10.1073/pnas.2119434119

[27] - Talà, Lorenzo et al. “Pseudomonas aeruginosa orchestrates twitching motility by sequential control of type IV pili movements.” *Nature microbiology* vol. 4,5 (2019): 774-780. doi:10.1038/s41564-019-0378-9

[28] - Kühn, Marco J et al. “Mechanotaxis directs *Pseudomonas aeruginosa* twitching

motility.” *Proceedings of the National Academy of Sciences of the United States of America* vol. 118,30 (2021): e2101759118. doi:10.1073/pnas.2101759118

[29] - Craig, Lisa et al. “Type IV pilin structure and assembly: X-ray and EM analyses of Vibrio cholerae toxin-coregulated pilus and Pseudomonas aeruginosa PAK pilin.” *Molecular cell* vol. 11,5 (2003): 1139-50. doi:10.1016/s1097-2765(03)00170-9

[30] - Wang, Fengbin et al. “Cryoelectron Microscopy Reconstructions of the Pseudomonas aeruginosa and Neisseria gonorrhoeae Type IV Pili at Sub-nanometer Resolution.” *Structure (London, England : 1993)* vol. 25,9 (2017): 1423-1435.e4. doi:10.1016/j.str.2017.07.016

[31] - Hannah Ochner et al. “Structure of the *Pseudomonas aeruginosa* PAO1 Type IV pilus.” bioRxiv 2024.04.09.588664. doi:10.1101/2024.04.09.588664

[32] - Avilan, Luisana. “Assembling Multiple Fragments: The Gibson Assembly.” *Methods in molecular biology (Clifton, N.J.)* vol. 2633 (2023): 45-53. doi:10.1007/978-1-0716-3004-4_4

[33] - Chibeu, Andrew et al. “The adsorption of Pseudomonas aeruginosa bacteriophage phiKMV is dependent on expression regulation of type IV pili genes.” *FEMS microbiology letters* vol. 296,2 (2009): 210-8. doi:10.1111/j.1574-6968.2009.01640.x

[34] - Lavigne, Rob et al. “A multifaceted study of Pseudomonas aeruginosa shutdown by virulent podovirus LUZ19.” *mBio* vol. 4,2 e00061-13. 19 Mar. 2013, doi:10.1128/mBio.00061-13

[35] - Craig, L., Forest, K.T. & Maier, B. Type IV pili: dynamics, biophysics and functional consequences. *Nat Rev Microbiol* 17, 429–440 (2019). doi:10.1038/s41579-019-0195-4

[36] - Aramaki, H, and M Fujita. “In vitro transcription analysis of rpoD in Pseudomonas aeruginosa PAO1.” *FEMS microbiology letters* vol. 180,2 (1999): 311-6. doi:10.1111/j.1574-6968.1999.tb08811.x

[37] - Thongchol, Jirapat et al. “Removal of *Pseudomonas* type IV pili by a small RNA virus.” *Science (New York, N.Y.)* vol. 384,6691 (2024): eadl0635. doi:10.1126/science.adl0635

[38] - Hartmann, Raimo et al. “BacStalk: A comprehensive and interactive image analysis software tool for bacterial cell biology.” *Molecular microbiology* vol. 114,1 (2020): 140-150. doi:10.1111/mmi.14501

[39] - https://github.com/AnjaliPattathil/AnalysisScripts